

ShapeSearch: A Flexible and Efficient System for Shape-based Exploration of Trendlines

Tarique Siddiqui, Zesheng Wang, Paul Luh, Karrie Karahalios, Aditya Parameswaran

University of Illinois (UIUC)

{tsiddiq2,zwang180,luh2,kkarahal,adityagp}@illinois.edu

ABSTRACT

Identifying trendline visualizations with desired patterns is a common and fundamental data exploration task. Existing visual analytics tools offer limited *flexibility* and *expressiveness* for such tasks, especially when the pattern of interest is under-specified and approximate, and do not scale well when the pattern searching needs are ad-hoc, as is often the case. We propose ShapeSearch, an efficient and flexible pattern-searching tool, that enables the search for desired patterns via multiple mechanisms: sketch, natural-language, and visual regular expressions. We develop a novel *shape querying algebra*, with a minimal set of primitives and operators that can express a large number of ShapeSearch queries, and design a natural-language and regex-based parser to automatically parse and translate user queries to the algebra representation. To execute these queries within interactive response times, ShapeSearch uses a fast shape algebra-based execution engine with query-aware optimizations, and perceptually-aware scoring methodologies. We present a thorough evaluation of the system, including a general-purpose user study, a case study involving genomic data analysis, as well as performance experiments, comparing against state-of-the-art time series shape matching approaches—that together demonstrate the usability and scalability of ShapeSearch.

1 INTRODUCTION

Identifying patterns in trendlines or line charts is an integral part of data exploration—routinely performed by domain experts to make sense of their datasets, gain new insights, and validate their hypotheses. For example, clinical data analysts examine trends of health-indicators such as temperature and heart-rate for diagnosis of medical conditions; astronomers study the variation in properties of galaxies over time to understand the history and makeup of the Universe; biologists analyze gene expression patterns over time to study biological processes; and financial analysts study patterns in stock trends data to predict future behaviour.

Lacking extensive programming experience, these domain experts typically perform manual exploration, tediously examining visualizations one at a time until they find those that match their desired shape or pattern.

An alternative approach is to use visualization tools that let them interactively search for desired patterns [8, 29, 44]. However, these tools are *limited and overly rigid*, and are therefore unable to support search when the desired shape is complex, or when the shape is under-specified or approximate, e.g., finding a product whose sales is decreasing for

some time, followed by a sharp rise, where the position and intensity of movements is left unspecified. Some data mining tools provide the ability to search for patterns in time series, e.g., [15, 34], but require heavy precomputation and indexing, limiting ad-hoc exploration, in addition to suffering from the same limitations in flexibility as the visualization tools. Yet another alternative for domain experts with programming expertise is to write code to perform this flexible match, but writing code for each new use-case and manually optimizing them can quickly become as tedious as manual searching of visualizations to find patterns.

We present ShapeSearch, a visual data exploration system that supports multiple novel mechanisms to express and effortlessly search for desired patterns in trendlines. Before describing ShapeSearch, we highlight the key characteristics of pattern matching tasks, along with real-world examples that motivated the design of ShapeSearch:

Blurry Patterns. Domain experts typically search for patterns that are “approximate”, and are often not interested in the specific details as much as the overall shape. We call such approximate patterns as *blurry* patterns. For example, biologists routinely look for structural changes in gene expression, e.g., rising and falling at different times (Figure 1a). Structural changes characterize internal biological processes such as the cell cycle or circadian rhythms, or external perturbation, such as the influence of a drug or presence of a disease. For instance, distinct patterns of gene expressions depicted during the mammalian embryonic development correlate with the differentiation of organs including the nervous system, liver, skin, lungs, and the digestive system, providing insight into the mechanisms of mammalian development, as well as the evolution of developmental processes [46].

Expressive and Flexible. Pattern matching tasks often go beyond finding a sequence of patterns, requiring arbitrary combinations (e.g., disjunction, conjunction or quantifiers) with varying location or width constraints. Examples include finding stocks with at least 2 peaks within a span of 6 months (e.g., double top, triple top patterns that indicate future downtrends [1]) or finding cities where the temperature rises from November to January and falls during May to July (e.g., Sydney).

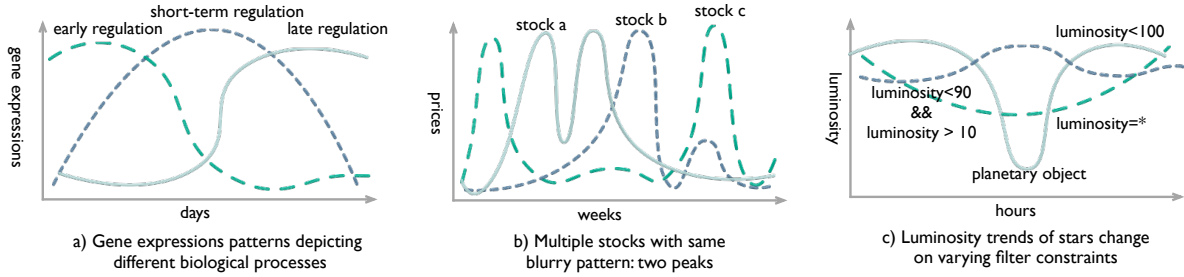


Figure 1: Shapes characterizing various real world phenomena

Ad hoc and Interactive. Pattern matching tasks operate over visualization collections that are defined *on-the-fly* during analysis. For example, astronomers monitor the brightness (luminosity) of stars over time to search for new planetary objects—a dip in brightness is symbolic of a planetary object passing between the star and the telescope, and the width and the degree of dips are used for characterizing these planetary objects [30]. Based on their domain understanding, astronomers apply *on-the-fly* filters (on values, specific attributes, and so on), or modify the scale (e.g., from seconds to days to months) to change the shape of the trend (Figure 1c). Moreover, often the actual patterns being explored are not known in advance, but are discovered during exploration. For instance, biologists often search for a pattern in a group of genes, that is similar to a pattern just discovered in another group (Section 8).

Contributions. To satisfy the three desired characteristics, ShapeSearch incorporates (a) an expressive shape query algebra, that can be invoked via (b) multiple flexible shape query specification mechanisms, and a (c) scalable pattern execution engine to execute shape queries within interactive response times.

(a) The *shape query algebra* abstracts key shape-based primitives and operators, for expressing a large variety of patterns in trendlines. We developed this algebra after many discussions with domain experts, including astronomy and genomics, as well as studying a large corpus of pattern queries collected via Mechanical Turk.

(b) ShapeSearch supports multiple specification mechanisms that are internally translated to a shape query algebra representation: ShapeSearch supports a *natural language interface*, coupled with a sophisticated parser and translator for translating them into the algebra. Unlike structured query languages, users do not need to know the syntax and semantics of the internal representation. However, one obvious downside is that natural language queries are often imprecise with ambiguous interpretation and missing details. ShapeSearch, therefore, leverages a mix of learning- and rule-based automated as well as user-driven ambiguity resolution mechanisms to tackle these issues. Additionally, ShapeSearch supports a *sketching interface* for simpler patterns, and returns

visualization that precisely match the drawn trends. To support more complex needs, the system provides a *visual regular expression* language for issuing queries that cannot be easily expressed via natural language or sketching. The three interfaces can be used simultaneously and interchangeably, as user needs and pattern complexities evolve.

(c) For supporting interactive response times on ad-hoc queries, ShapeSearch leverages a pattern-matching engine that relies on minimal pre-processing or indexing. Directly generating and processing a large collection of visualizations, where each visualization has thousands of values, can lead to a long response time. Instead, ShapeSearch uses a *pipelined-execution model*—with *perceptually-aware* pattern scoring mechanisms and *query-aware* optimizations—that help prune a large number of visualizations and/or parts of visualizations, for effective and efficient pattern matching.

Relationship with Existing Work. ShapeSearch builds upon a number of prior papers from the data-mining and visualization communities, each of which lacks at least one of the three desired characteristics outlined above. Visual querying tools [29, 31, 34, 40, 44, 47] allow users to search for trendlines by taking the sketch of the desired shape as an input along with soft or hard constraints on trendline values, but lack sufficient querying expressiveness for searching for complex shapes involving *blurry* patterns as well as multiple x , y , or *width* constraints at the same time. In addition, these tools usually leverage distance measures [33, 36] that compare two trends based on their values, and are therefore more suited for scenarios where the input query is a trendline (or a portion of it) from the same domain as target visualizations. As we will show, these measures are not appropriate when explicitly searching for characteristics of the trendline, and instead get overwhelmed by noise. There are some regular-expression- [34] or keyword-based [15] tools for pattern searching in sequence databases. Trendlines in these tools are abstracted using a few symbols, often indexed in advance. As a result, these tools offer limited expressivity and flexibility when it comes to on-the-fly ad-hoc pattern queries. There are a few natural language-based tools for querying databases [27] and generating visualizations [14, 42]. However, the parsing and translation strategies in ShapeSearch

are based on our ShapeQuery algebra, and therefore substantially differ from these tools. We provide more detailed comparisons with related work in Section 10.

Outline. We first describe the ShapeSearch system (Section 2) followed by the ShapeQuery algebra (Section 3), comprising the primitives and operators that help express a wide variety of use-cases. Next, we describe how we translate natural language queries into a structured ShapeQuery representation (Section 4). We explain the ShapeSearch execution engine (Section 5), and optimizations (Section 6). We present a user study (Section 7) and a genomics case study (Section 8), focusing on evaluating the expressiveness, effectiveness, and usability of ShapeSearch, as well as a performance experiments evaluating the efficiency and accuracy of ShapeSearch pattern execution engine (Section 9).

2 SYSTEM OVERVIEW

ShapeSearch provides powerful yet flexible mechanisms for users to search for trendline visualizations with a desired shape. In this section, we first present an overview of the front-end interface and user experience, and then describe the back-end.

Front-end. ShapeSearch supports an interactive interface for composing shape queries, as well as for displaying the result visualizations. Figure 2 depicts this interface, with an example query on genomics data discussed in the introduction. Here, the user is interested in searching for genes that get suppressed due to the influence of a drug, depicted by a specific shape in their gene expression — first rising, then going down, and finally rising again — with three patterns: up, down, and up, in a sequence. To search for this shape, the user first loads the dataset [7]), via form-based options on the left (Figure 2 Box 1), and then selects the space of visualizations to explore by setting the x axis as time, the y axis as expression values, and the category as gene. Each value of the category attribute results in a candidate visualization with the given x and y axis. Thus, the category attribute defines the space of visualizations over which we match the shape. ShapeSearch supports three mechanisms for shape specification — natural language, regular expressions (regex for short), and sketching on a canvas:

Sketching on Canvas. By drawing the desired shape as a sketch on the canvas (Figure 2 Box 2a), the user can search for visualizations that are *precisely* similar (using a distance measure such as Euclidean distance or Dynamic Time Warping [36]). As soon as the user finishes sketching, ShapeSearch outputs visualizations that are precisely similar to the drawn sketch in the results panel (Figure 2 Box 4).

Natural Language (NL). For searching for visualizations that approximately match patterns, users can use natural language. For instance, as in Figure 2 Box 2b, the desired shape in the aforementioned genomics example can be expressed as “show me genes that are rising, then going down, and then

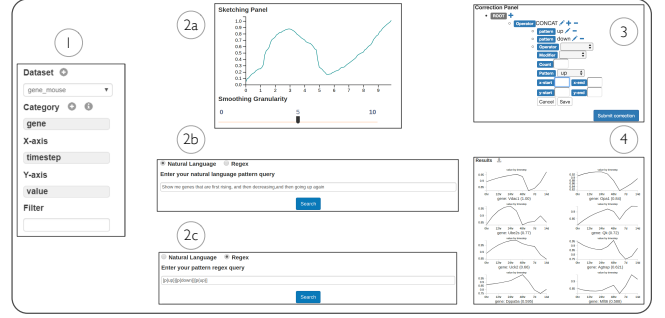


Figure 2: ShapeSearch Interface, consisting of six components. 1) Data upload, attributes selection, and applying filter constraints 2) Query specification: 2a) Sketching canvas 2b) Natural language query interface, and 2c) Regular expression interface, 3) Correction panel, and 4) Results panel

increasing”. Similarly, scientists analyzing cosmological data can easily search for supernovae (bright stellar explosions) using “find me objects with a sharp peak in luminosity”. We describe in Section 4 how ShapeSearch translates natural language queries to a structured internal representation.

Regular Expression (regex). For queries that involve complex combinations of patterns that are difficult to express using natural language or sketch, the user can issue a regular expression-like query that directly maps to the structured internal representation, consisting of ShapeSearch primitives and operations, described in detail in Section 3.

During exploration, users can choose specification mechanisms interchangeably based on the complexity of the query. For both NL as well as regex, ShapeSearch, additionally supports auto-complete functionality to guide users towards their target query. All queries are issued to the back-end using a REST protocol. We use the term *user query* to refer to the submitted query using any of the specification mechanisms.

Back-end. Figure 3 depicts the back-end components of ShapeSearch. The back-end parses and translates the user query into a ShapeQuery, a structured internal representation of the query consisting of operators and primitives supported in our algebra (Section 3). The back-end supports an ambiguity resolver that uses a set of rules for automatically resolving syntactic and semantic ambiguities, as well as forwards the parsed query to the user for further corrections and validation (Figure 2 Box 3). The validated query is finally optimized and executed by the execution engine (Section 5), and the top visualizations that best match the ShapeQuery are presented to the user in the results panel (Figure 2 Box 4).

3 SHAPE QUERY ALGEBRA

In this section, we describe the ShapeQuery algebra, a structured internal representation of a user query, supporting a minimal set of primitives and operators that capture a wide

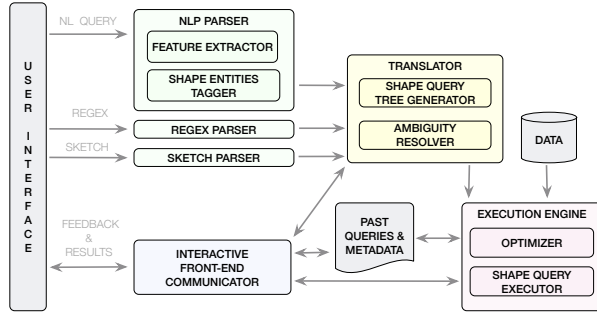


Figure 3: System Architecture.

range of ShapeSearch use-cases. Each user query issued at the front-end is automatically translated into a ShapeQuery, which is then optimized and executed by the execution engine.

The most interesting feature of ShapeQuery is its capability for “blurry” matching, allowing users to search for major changes in trendlines instead of local perturbations, fluctuations, or noise. For example, biologists are often interested in locating genes whose expressions first fall and then rise, or ones that rise at least twice but fall not more than once over a duration of 4 weeks. Here, they expect the system to ignore any minor fluctuations over a small window of one or two days (which may occur due to temporary cell mechanisms), and rather capture the major changes, that can happen due to the influence of an external agent such as a drug. The ShapeQuery algebra makes it natural to express such queries. Another important feature of ShapeQuery is that it has been designed to be efficiently executed within interactive response times. We describe the execution engine and optimizations in Sections 5 and 6.

For efficient and blurry matching of pattern search queries, ShapeSearch represents a shape as a combination of one or more patterns (e.g., rising followed by falling), where each pattern is matched over a sub-region of a visualization.

We call the part of query describing an individual pattern, as a ShapeSegment (S). Multiple patterns are captured by combining ShapeSegments using one or more *operators*. For example, one can search for two or more patterns in a sequence, two or more patterns matching the same sub-region of the visualization, or one of many patterns matching in a given sub-region of the visualization, among other possible combinations that we discuss shortly.

As an example, a user query “rising from $x=2$ to $x=5$ and then falling” can be translated into a ShapeQuery consisting of two ShapeSegments: $[x.s = 2, x.e = 5, p=up] \otimes [p=down]$. The first ShapeSegment captures “rising from $x = 2$ and $x = 5$ ”, and the second ShapeSegment expresses a “falling” pattern. Moreover, the second ShapeSegment must “follow” the first one, i.e., the “falling” sub-region of the visualization must start from the end point of the region where “rising”

is matched ($x=5$). As we will see in a bit, such a sequence is captured using CONCAT operator denoted by \otimes .

Next, we describe the shape primitives and operators that constitute the ShapeQuery algebra. Table 1 lists these primitives and operators.

3.1 Shape Primitives

A shape can be described using five primitives — LOCATION (l), PATTERN (p), MODIFIER (m), ITERATOR ($.$), and POSITION ($\$$). ShapeSearch allows users to be vague or fuzzy about their intended shape, by skipping one or more of these primitives in their query. For example, users can skip the LOCATION values, if they want to match a PATTERN anywhere in the trendline. Similarly, users can input the exact trendline to match, or the endpoints of the ShapeSegments to match without specifying the PATTERN. Next, we describe each of the supported primitives.

LOCATION (l) defines the endpoints of the sub-region of the visualization between which a pattern is matched. It consists of four sub-components, not all of which are mandatory: starting X coordinate ($x.s$), starting Y coordinate ($y.s$), ending X coordinate ($x.e$), ending Y coordinate ($y.e$). For example, $[x.s = 2, x.e = 10, y.s = 10, y.e = 100]$ is a simple ShapeQuery for finding visualizations whose trend between $x=2$ to $x=10$ is similar to the line segment starting at (2, 10) and ending at (10, 100).

PATTERN (p) defines a trend or a semantic feature in a sub-region of the visualization. The system supports a set of basic semantic patterns, commonly used for characterizing trendlines, such as *up*, *down*, *flat*, or the slope (θ) in degrees. For example $[p=up]$ finds trendlines that are increasing, $[p=45]$ finds trendlines that are increasing with a slope of about 45° , and $[x.s=2, x.e=10, p=up]$ finds trendlines that are increasing from $x = 2$ to 5. Users can also define their own domain-specific User-Defined Pattern (*udp*), and use it in the ShapeQuery along with other shape primitives. Like other declarative systems, ShapeSearch treats *udp* as black-boxes, and does not perform any optimization during their execution. We describe in more detail how ShapeSearch matches patterns in Section 5.

SKETCH (v). In addition to semantic patterns, users can also draw a sketch in order to find visualizations that are precisely similar to the drawn sketch, a functionality that is also supported in visual query systems [8, 29, 44]. ShapeSearch automatically translates the pixel values of the user-drawn sketch to the domain values of the X and Y attributes, and adds the transformed vector of (x,y) values as v in the ShapeQuery. As an example, the ShapeQuery $[v=(2:10,3:14, ...,10:100)]$ finds the visualizations that have precisely similar values to that of v in the query using a distance measure such as Euclidean distance, or Dynamic Time Warping [36].

MODIFIER (m) further refines the way a semantic pattern is matched. For example, one can ask for trendlines that rise sharply or ones that have at least two peaks. On combining $m = \gg$ with $p=up$, one can search for trends that rise sharply. Similarly, $m = 2$ can be combined with $p=up$ to find trendlines that rise twice; $m = \{2, 5\}$ refers to the occurrence of a pattern between 2 and 5 times; $m = \{2, \}$ refers to at least 2 times; and $m = \{, 2\}$ refers to at most 2 times. MODIFIER, when used along with the POSITION operator (described later) can help compare a ShapeSegment with previous or subsequent ShapeSegments in the query (e.g., the slope of second ShapeSegment must be more than that of the first ShapeSegment, or rise by at least 2X relative to that of the first ShapeSegment).

ITERATOR ($.$) is a powerful sub-primitive that can be used along with the LOCATION sub-primitives to iterate or scan over the points in the trendline to match a desired pattern repetitively. For example, one can search for cities with maximum rise in temperature over a width of 3 months using query: $[x.s = ., x.e = (. + 3), p=up]$. Here the ITERATOR ($.$) iterates over all points in the trendline, setting each point as the start x position, with the x end position set to the point that is 3 points ahead.

POSITION ($\$$) is another useful sub-primitive that can be used within PATTERN primitive in one ShapeSegment to refer to the pattern in other ShapeSegments (either previous or subsequent). Along with POSITION, MODIFIER can be set to $>$, $<$, or $=$ to ensure that the slope of the pattern in the current ShapeSegment is more than, less than or equal to the slope of the pattern in the referred ShapeSegment. For example, astronomers can issue a simple ShapeQuery $[p=up][p=\$0, m=<]$ with $x=$ time and $y=$ luminosity (brightness) to search for celestial objects that were initially moving fast towards earth, but after some point either slowed down or started moving away from the earth. The second ShapeSegment $[p=\$0, m=<]$ ensures that the rate of brightness is less than that in the first part of the visualization $[p=up]$, indicating that the object has started moving either slower than before, or away from the earth. In addition, one can set $m = < \frac{1}{2}$ to ensure the slope of second part is at most (1/2) of the first part. Similarly, $\$-$ and $\$+$ can be used to refer to the previous or the subsequent ShapeSegments respectively.

3.2 Operators

So far, we have seen examples of ShapeQueries with a single ShapeSegment. Now, we will see how we can use operators to combine multiple ShapeSegments to search for complex shapes. We support five operators.

MATCH ($[]$) is a unary operator that takes as input a ShapeSegment, executes it over one or more sub-regions (visual segments) of the visualization. As a rule, every ShapeSegment is bounded to the MATCH operator.

CONCAT (\otimes) specifies a sequence of two or more ShapeSegments. For example, one can search for genes that are first rising, and then falling.

AND (\odot) simultaneously matches two or more patterns in the same sub-region of the visualization. Unlike CONCAT, all of the patterns must be present in the same sub-region of the visualization. For example, one can look for genes whose expression values rise twice but do not fall more than once within the same sub-region.

OR (\oplus) searches for one among many patterns in the same sub-region of the visualization, picking the one that matches the sub-region the most. For example, one can search for genes whose expressions are either *up*-regulated or *down*-regulated.

OPPOSITE ($!$). A unary operation for matching the opposite of the shape expressed in the ShapeSegment. For example, instead of saying increasing or decreasing pattern, one can say not *flat* pattern.

Grouping and Nesting. ShapeSegments can be grouped to specify precedence of some sub-expressions of the query over others. For example, one can search for genes whose expression values were “first increasing and then either stabilized, or decreased and then increased again”. In order to ensure that only one of the patterns “*flat*” (stable) or “*down then up*” is used in the second part of the query, one can use parenthesis ($()$) to indicate precedence: $[p=up] \otimes ([p=flat] \oplus ([p=down] \otimes [p=up]))$

Similarly, ShapeSearch allows ShapeSegments to be *nested* as a value for PATTERN primitive to search for complex shapes. For example, one can use nesting to search for stocks that increased and then went *down* within a span of 4 weeks anytime between the months of Feb and October, using the following query $[x.s = 2, x.e = 10, p=[x.s=., x.e = . + 4, p=[[p=up][p=down]]]]$.

Regular expression and sketch-based queries can be directly parsed into an Abstract Syntax Tree (AST) (depicted in Figure 4) using the context-free grammar (Table 2). For natural language queries, however, ShapeSearch additionally needs to identify the words (i.e., non-noise words) corresponding to the shape primitives and operators as well as effectively resolve ambiguities for constructing meaningful and consistent AST representations.

4 PARSING AND TRANSLATION

We, now, give a brief overview of the steps involved in natural language parsing and translation

Shape Primitives and Operators Recognition. A natural language query consists of a sequence of words, where each word either maps to one of the entities (primitives and operators) in the ShapeQuery, or is a noise word. We follow a two-step process in identifying and tagging words corresponding to shape primitives and operators (together

Table 1: Primitives and Operators in ShapeQuery Algebra

Symbol	Name	Type
L	LOCATION	Primitive
$x.s$	START X VALUE	Location Sub-Primitive
$y.s$	START Y VALUE	Location Sub-Primitive
$x.e$	END X VALUE	Location Sub-Primitive
$y.e$	END Y VALUE	Location Sub-Primitive
$.$	ITERATOR	Location Sub-Primitive
p	PATTERN	Primitive
num	SLOPE	Pattern value
up	UP	Pattern Value
$down$	DOWN	Pattern Value
$flat$	FLAT	Pattern Value
udp	USER-DEFINED PATTERN	Pattern Value
$\$$	POSITION	Pattern Sub-Primitive
v	SKETCH	Primitive
m	MODIFIER	Primitive
$>$	MORE or GRADUAL UP	Modifier value
$>>$	MUCH MORE or SHARPER UP	Modifier value
> 2	ATLEAST 2X	Modifier value
$=$	SIMILAR	Modifier value
$<$	LESS or GRADUAL DOWN	Modifier value
$<<$	MUCH LESS / SHARPER DOWN	Modifier value
$[]$	MATCH	Operator
\otimes	CONCAT	Operator
\odot	AND	Operator
\oplus	OR	Operator
$!$	OPPOSITE	Operator

Table 2: ShapeQuery Context Free Grammar

Q	$\rightarrow Q \otimes S Q \odot S Q \oplus S !Q (Q)$
S	$\rightarrow [(L,)^+(P,)^+(M,)^+ V^+]$
L	$\rightarrow (x.s = num,)^+(x.e = num,)^+(y.s = num,)^+(y.e = num,)^+$ $\rightarrow (x.s = ., x.e = . + num)$
P	$\rightarrow (p = up down flat num \$num udp S)$
M	$\rightarrow m = \{num^+, num^+\} < num^+ > num^+ >> << =$
V	$\rightarrow (num : num,)^*$

called entities). First, based on the Part-of-Speech (POS) tags and word-level features, we classify each word in the query as either noise or non-noise. For example, words $\in \{\text{determiner, preposition, stop-words}\}$ are more likely to be noise, while words $\in \{\text{noun, adjective, adverb, number, transition words, conjunction}\}$ may refer to one of the entities — almost all the entities in our training corpus (described in a bit) had one of these POS Tags. Next, given a sequence of non-noise words, we use a linear-chain conditional-random field model (CRF) [25] (a probabilistic graphical model used for modeling sequential data, e.g., POS tagging) to predict their corresponding entities. To train the CRF model, we extract a set of features (listed in Table 3) for each non-noise word in the sequence. While noise words are not part of the sequence, they are still used for deriving features for the non-noise words. In addition, ShapeSearch stores a list of frequently occurring words, called “synonyms”, for each entity type (e.g., “increasing” for up, “next” for CONCAT), and if a non-noise words matches closely (e.g., with edit distance ≤ 2) with one of these synonyms, we add the matched entity-type as a feature named predicted-entity. This idea is inspired from

Table 3: Features used during natural language parsing ($d(x)$ denotes distance in terms of number of words between current word and x), $x+$ denotes next x , $x-$ denotes previous x .

Type	Features
POS Tags	pos-tag, pos-tag-, pos-tag+
Words	word-, word+, word-, word++
Predicted entities	predicted-entity, predicted-entity+, predicted-entity-, d(predicted-entity+), d(predicted-entity-)
Space and time prepositions	time-preposition+, time-preposition-, space-preposition+, space-preposition-, d(time-preposition+), d(time-preposition-), d(space-preposition+), d(space-preposition-)
Punctuation	d(+), d(-), d(+), d(-), d(+), d(-)
Conjunctions	d(and+), d(or-), d(and then+)
Miscellaneous	d(x), d(y), d(next), ends(ing), ends(ly), length(query)

the concept of “bootstrapping” in weakly-supervised learning approaches [24, 45], and helps improve the overall accuracy. For training the CRF model, we collected and tagged 250 natural language queries via Mechanical Turk, where crowd workers were asked to describe patterns in trendline visualizations using at most three sentences. We implemented the model using the Python CRF-Suite library [3] with parameter settings: *L1 penalty:1.0, L2 penalty:0.001, max iterations: 50, feature.possible-transitions: True*. On cross-validation, the model had an F1 score of 81% (*precision = 73%, recall = 90%*).

Identifying Pattern and Modifier Value. For the words predicted as of type PATTERN or MODIFIER, we map them to one of the supported values (e.g., up, down, more, less, sharp, much more, etc.) with the help of synonyms. In particular, ShapeSearch first calculates the normalized edit distance, i.e., edit distance/(average length of the two words), between the word and each of the synonyms of a supported value, and takes the minimum. If the lowest edit distance across all values is more than a threshold (.1 as default), ShapeSearch further calculates the average semantic similarity (using wordnet synset [39]) between the entity and the synonyms of each value, and finally selects the value with highest similarity score.

ShapeQuery Tree Generation. After identifying primitives and operators, we use a context-free grammar [9] depicted in Table 2 to construct an AST (depicted in Figure 4). Note that the same CFG is also used for parsing regex and sketch. However, natural language translation often incurs syntactical and semantic ambiguities. In the presence of syntactical ambiguities, the parser fails to construct a unique AST representation using CFG rules, while semantic ambiguities may lead to ASTs that are not meaningful (e.g., increasing from $y=10$ to $y=5$).

Ambiguity Resolution. Ambiguities mainly arise from a) wrong entity type matching, b) grouping of entities into ShapeSegments, or c) incorrect sentence structures, often

Table 4: Common Ambiguities and their Resolution

Ambiguity (example queries with predicted entites)	Resolution
Multiple p in the same ShapeSegment (e.g., [increasing(p) from 2($x.s$) to 5($x.e$) decreasing(p)] next (\otimes) [sharply (m)])	Move one of the p to the adjacent ShapeSegment with missing p , else split the ShapeSegment into two new ShapeSegments with an OR operator between them
ShapeSegment with m but no p (see example above)	Move the m in the current ShapeSegment to the adjacent ShapeSegment with p but missing m , else ignore ShapeSegment with m
Conflicting l and p in a ShapeSegment (e.g., [decreasing(p) from 4($x.s$) to 8($x.e$)])	Change the sub-primitive of l from x to y or y to x , else swap the start and end positions.
Overlapping ShapeSegments with \otimes (e.g., increasing(p) from 4($x.s$) to 8($x.e$) and then (\otimes) decreasing(p) from 8($x.s$) to 0($x.e$))	Change x to y , if y values missing. If y values already present, replace \otimes with \odot operator.

caused due error in usage of punctuation or transition words. To resolve ambiguities, we first group all shape primitive entities between two operator entities into one ShapeSegment, and apply rule-based transformations to the structure, that reorder and change the types of entites until we get a correct and meaningful AST. We list some of the commonly seen ambiguities and their resolution in Table 4.

Parsed ShapeQuery Validation. The parsed ShapeQuery is sent to the front-end, and displayed as part of the correction panel (Box 4 in Figure 2) for users to correct, further refine or edit the query if needed. The correction panel is a form-based representation of the ShapeQuery, where users can add, delete, or modify ShapeQuery primitives and operators with the help of drop-down menu options, or filling in text-boxes. While the ShapeQuery is validated by the user, the system executes the parsed query in parallel, and resulting visualizations are displayed in the result panel. If the users choose to modify the ShapeQuery, the validated query is executed again and results are updated.

5 QUERY EXECUTION

After the user submitted query is parsed, translated, and validated, the Abstract Syntax Tree (AST) representation (depicted in Figure 4) of the ShapeQuery is sent to the execution engine. The execution engine generates visualizations from the dataset, and evaluates them to select the top k visualizations that best match the desired shape. We begin by formally describing the problem setting.

5.1 Shape Matching Problem

Like other data exploration systems, the ShapeSearch execution engine considers a traditional OLAP data exploration setting with dataset (D), stored in either a database, or as a raw file in CSV or JSON. The execution engine takes as input ShapeQuery (Q) as an AST and visual parameters (R), both parsed and translated from user input. R primarily consists of z , x , and y attributes that together specify the space of visualizations of interest for matching. The x and y attributes specify the attributes used for the x - and y - axes, while the z attribute corresponds to multiple visualizations, one for each unique z value. For example, z =‘product’, x =‘year’ and y =‘sales’ corresponds to multiple trendlines, one for each product, with x axis as year, and y axis as sales. Users can also

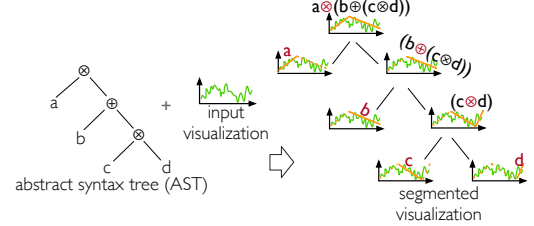


Figure 4: Segmenting a visualization according to input ShapeQuery

specify filter constraints (f), binning width (b), and aggregation (a) for reducing the number of points before generating trendlines.

The ShapeSearch execution engine generates a collection of visualizations called *candidate visualizations* V , based on R (i.e., $V \in \text{gen}(R)$), and assigns a score sc_i to each candidate $V_i \in V$ using a scoring function SF that captures how closely it matches the ShapeQuery Q . The top k visualizations with highest scores are returned. Formally,

Problem 1. Given a dataset D , a ShapeQuery Q , visual parameters R , and a scoring function SF , find top k visualizations V_1, V_2, \dots, V_k that maximize $SF(Q, V_i)$, from all $V \in \text{gen}(R)$.

We first explain our scoring methodology, and then describe the query execution pipeline that ShapeSearch uses for generating and scoring candidate visualizations. In the next section, we discuss how ShapeSearch optimizes the execution of fuzzy ShapeQueries— i.e., ShapeQueries with missing LOCATION primitives, which constitute a large fraction of user queries. As we will see later, for fuzzy ShapeQueries, ShapeSearch has to automatically find the optimal location values for ShapeSegments, among all of the points in the visualization.

5.2 Scoring

For scoring, ShapeSearch segments each candidate visualization V_i into multiple sub-regions, depending on the ShapeSegments and the operators in the ShapeQuery. We use the term SegmentedViz to denote a candidate visualization that is segmented into one or more sub-regions, with a sub-region in the SegmentedViz being called VisualSegment.

Figure 4 depicts how a candidate visualization is segmented for a ShapeQuery $a \otimes (b \oplus (c \otimes d))$, representing

Table 5: Scoring Patterns

Pattern	Score
<i>up</i>	$\frac{2 \cdot \tan^{-1}(\text{slope})}{\pi}$
<i>down</i>	$-\frac{2 \cdot \tan^{-1}(\text{slope})}{\pi}$
<i>flat</i>	$(1.0 - \ \frac{4 \cdot \tan^{-1}(\text{slope})}{\pi}\)$
$\theta = x$	$(1.0 - \ \frac{2 \cdot \tan^{-1}(\text{slope} - x)}{(\pi - \ \tan^{-1}(x)\)}\)$
$*$	1
<i>empty</i>	-1
v	L_2 norm (configurable)

a shape with a ShapeSegment a in the beginning followed by either ShapeSegment b , or a sequence of two ShapeSegments c and d . As depicted in the right side of the figure, CONCAT (\otimes) at the root segments the visualization into two VisualSegments: the first VisualSegment is used for scoring ShapeSegment a , while the second segment is for scoring sub-expression $(b \oplus (c \otimes d))$. Traversing down the AST, we see the OR (\oplus) operator between b and $(c \otimes d)$, that scores the two sub-expressions independently on the second VisualSegment. However, for scoring $c \otimes d$, the second VisualSegment is further split into two segments.

The SegmentedViz is scored bottom-up, starting with VisualSegments corresponding to leaf ShapeSegments in the AST (e.g., a , b , c , and d). The scores vary from 1.0 (best match) to -1.0 (worst match), based on how closely the ShapeSegments match the VisualSegments. After leaf nodes, scores of the intermediate nodes (operators) are computed by combining the scores of children nodes according to the definitions of operators, that we discuss shortly. The score of the root operator corresponds to the overall score of the SegmentedViz. Now, we discuss the scoring functions.

Scoring a ShapeSegment. The score of a ShapeSegment depends on two parts. The first part dictates whether the VisualSegment satisfies the LOCATION primitive, and any other constraints specified as part of the MODIFIER in ShapeQuery. When the LOCATION primitives are not satisfied, we assign an overall score of -1 (i.e., the least possible score) to the ShapeSegment, and ignore the second part.

The second part captures how similar the VisualSegment is to the PATTERN primitive in the ShapeSegment. For computing this part, we focus on *efficacy* and *efficiency*. By *efficacy*, we mean the scoring should be able to capture the key trend in the VisualSegment while ignoring any local fluctuations if any. At the same time, the score should be *efficiently* computable within interactive response times. ShapeSearch, therefore, approximates each VisualSegment with a *line segment*, and uses features of this line segment, such as slope, for computing scores, as described below. We represent complex non-linear shapes using multiple line segments that ShapeSearch can automatically infer from the user-drawn sketch, or can be specified via a regex.

Table 5 depicts the scoring functions for each of the supported pattern types. The scoring functions are based on the following observation: we notice that a pattern or a trend

Table 6: Scoring Operators. sc denotes the score of a ShapeSegment.

Operator	Score
CONCAT	$\frac{(sc_1 + sc_2 + \dots + sc_k)}{k}$
AND	$\min(sc_1, sc_2, \dots, sc_k)$
OR	$\max(sc_1, sc_2, \dots, sc_k)$
NOT	$-(sc)$

can have multiple ways of depicting itself. For example, all VisualSegments with slopes from 0° to 90° have *up* patterns, and should have scores > 0 . Moreover, a VisualSegment with a slope of 80° has a better *up* pattern than the one with a slope of 30° , thus the score should increase as the slope of the VisualSegment increases, and vice-versa. On the other hand, a VisualSegment with a slope $< 0^\circ$ has an opposite of *up* pattern, and should have a negative score. More importantly, a change in slope from 10° to 30° is perceptually more noticeable than from 60° to 80° , in other words, *the value of improvement in a pattern diminishes with the increase in the score of the pattern*. This is essentially similar in principle to the *law of diminishing returns* [2], and is modeled using the \tan^{-1} function, variants of which have also been considered in prior work, e.g., [35]. Thus, the score for *up* increases from -1 to 1 as the slope of the VisualSegment increases from -90° to $+90^\circ$. We follow the same principle for other patterns. For *flat*, the score is +1 when the slope is 0° and decreases to -1 as slope increases to $+90^\circ$ or -90° . For pattern type $\theta = x$, the score is maximized when the slope of the segment is x° , and decreases to -1 as the deviation between the slope of the line segment and x° increases. In Section 7.3, we compare our scoring functions with the state-of-the-art shape matching approaches that are frequently used in visual querying systems.

For a shape input as a sketch, users sometimes intend to perform *precise* matching. For such ShapeSegments we compute the score using L2 norm (Euclidean distance) between the drawn sketch and the VisualSegment without fitting a line segment. The L2 norm can vary from 0 to ∞ , therefore we normalize the distance withing $[1, -1]$.

In addition to providing domain-specific pattern types (UDPs), ShapeSearch also allows users to override the default scoring methodology by letting them define their own scoring functions. For seamless integration, user-defined scoring functions must take a VisualSegment as input, and output a score within $[-1, 1]$.

Scoring operators. As depicted in Table 6, the scoring functions of operators define how the scores from children ShapeSegments are combined. CONCAT matches a sequence of patterns, taking average of the scores of ShapeSegments. AND matches multiple patterns in the same VisualSegment, and therefore to avoid any pattern not having a good match, it takes the minimum of all scores. On the other hand, OR picks the best matching pattern among many, by taking the maximum of all scores.

Scoring quantifiers. When a ShapeSegment has a quantifier such as *at least*, *at most*, *between*, we divide the VisualSegment into smaller sub-segments. By default, we vary the sub-segment length from 2, the minimum possible length, to the length of VisualSegment, and score the pattern over each of the sub-segments like we score a VisualSegment. Then, we count the number of sub-segments where there is

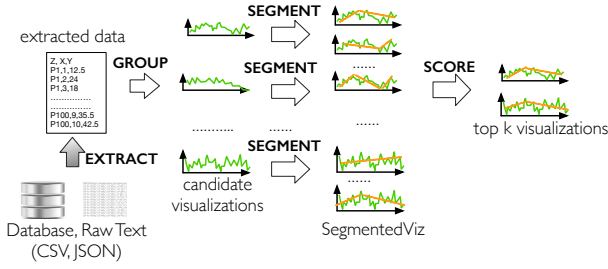


Figure 5: Query Execution Pipeline

a positive score (i.e., using zero as a threshold, which can be overridden by users). If the number does not satisfy the quantifier, we give the ShapeSegment a score of -1 , otherwise we calculate the score of the ShapeSegment by taking the average of scores across the minimum number of sub-segments that satisfy the constraint.

From the definitions of operators and quantifiers, we have:

Property 5.1 (Boundedness). *The absolute value of the score from an operator or quantifier is bounded between the minimum and maximum scores of the input ShapeSegments.*

This property will be useful in the later sections, where we discuss execution engine optimizations.

5.3 Pipelined Execution

In this section, we provide an overview of how ShapeSearch generates and scores visualizations given the visual parameters (R) and the ShapeQuery (Q). As depicted in Figure 5, ShapeSearch uses a *pipelining*-based execution model, where the execution is divided into a series of steps, each handled by an independent physical operator (represented by arrows). Pipelining helps improve the throughput of the system, and reduces the processing time by executing multiple operations simultaneously on a given visualization, taking advantage of the cache locality and improved CPU usage while reducing memory footprint. Here, we give a brief overview of the physical operators:

- 1) **EXTRACT** selects and aggregates records from the data source R (e.g., relational databases or raw text files) based on the z , x , y , filters (f), and aggregation (a) constraints, and sorts them on z and x attributes before streaming them to downstream operators.
- 2) **GROUP** generates visualizations, one corresponding to each unique value of the z attribute, and applies z -score normalization [16] if ShapeQuery has no constraints on y values. Each visualization is approximated using a sequence of small line-segments of length b , the binning width. If unspecified by the user, we set b to $(x \text{ range})/(\text{number of pixels along the } x \text{ axis})$, the minimum length of the time-series that users can discern at the front-end. As we will explain subsequently, downstream operators in the pipeline construct longer segments out of smaller segments during shape matching. GROUP passes only five numbers, called *summarized statistics*, for each line segment,

namely, $\sum x_i$, $\sum y_i$, $\sum x_i \cdot y_i$, $\sum x_i^2$, n ; substantially reducing the amount of data processed by the downstream operators. Moreover, these statistics are sufficient for downstream operators to estimate longer segments, without any loss of accuracy, as shown below.

Theorem 5.1 (Additivity). *Given two adjacent VisualSegments A and B , a line segment over the combined VisualSegment AB can be estimated using linear regression on the summarized statistics over the individual VisualSegments A and B .*

Proof: A line segment is characterized by slope θ and intercept δ , given by the following formulae:

$$\theta = \frac{(n \cdot \sum x_i \cdot y_i - \sum x_i \sum y_i)}{(n \cdot \sum x_i^2 - (\sum x_i)^2)}, \delta = \sum y_i - \theta * \sum x_i.$$

From these formulae, it is easy to see that:

$$\theta_{AB} = \frac{(n_A + n_B) * (\sum x_{Ai} \cdot y_{Ai} + \sum x_{Bi} \cdot y_{Bi}) - (\sum x_{Ai} + \sum x_{Bi}) * (\sum y_{Ai} + \sum y_{Bi})}{(n_A + n_B) * (\sum x_{Ai}^2 + \sum x_{Bi}^2) - (\sum x_{Ai} + \sum x_{Bi})^2},$$

$$\delta_{AB} = (\sum y_{Ai} + \sum y_{Bi}) - \theta_{AB} * (\sum x_{Ai} + \sum x_{Bi}).$$

Thus, the line segment over the combined region can be estimated using the summarized statistics over the individual regions. ■

Thus, the GROUP operator outputs a collection of visualizations, with each visualization consisting of an ordered list of summarized statistics. 3) **SEGMENT** takes approximated visualizations from GROUP as input, and as described in Section 5.2 segments each one into one or more segments according to the ShapeQuery, outputting one or more SegmentedVizs for each candidate visualization. We discuss in Section 6 the class of ShapeQueries for which the SEGMENT operator needs to consider multiple SegmentedVizs for a candidate visualization. 4) Finally, **SCORE** evaluates SegmentedVizs with respect to the ShapeQuery, and for each candidate visualization it assigns a score corresponding to the SegmentedViz with the maximum score, outputting top- k candidate visualizations with the highest scores.

Even a simple ShapeQuery often involves evaluation of a large number of visualizations, which can take many tens of seconds. Next, we discuss how ShapeSearch selectively pushes certain primitives within a ShapeQuery to the upstream operators to prune visualizations earlier in the pipeline, thereby reducing the overall query processing time.

5.4 Early Pruning via Push-Down

ShapeSearch employs three push-down optimizations to prune visualizations or parts of visualizations earlier in the query processing pipeline. We explain these optimizations below, with the help of the following ShapeQuery: $[p = \{up\}, x.s = 50, x.e = 100][p = \{down\}][p = \{up\}]$ — the query represents a shape which is *increasing* from 50 to 100 followed by a *down*, and then *increasing* pattern. (a) **LOCATION** primitives in ShapeQuery are pushed down to the **EXTRACT** to prune visualizations that do not have any value in the specified x ranges in the ShapeQuery (e.g., 50 to 100 in

the above query), **(b)** When a ShapeQuery contains a ShapeSegment with an *up* or *down* pattern along with both start and end locations (e.g., $[p = \{up\}, x.s = 50, x.e = 100]$ in the above query), the SEGMENT operator prioritizes the construction of VisualSegments over such location primitives first, and eagerly checks and discards visualizations with negative scores in these regions, thereby avoiding the creation and scoring of large number of false positive SegmentedVizs, and finally **(c)** GROUP avoids computing *summarized statistics* (discussed in the previous section) over x ranges not referred to in the ShapeQuery (e.g., 0 to 50 in the above query), since the values over such ranges are ignored for segmentation and scoring by the upstream operators. After scoring, however, for the top k visualizations, the values over the ignored x ranges are added back for plotting the complete visualizations at the front-end.

Overall, as we will see in Section 9, these push-down optimizations significantly help in improving the interactivity of the ShapeSearch system.

6 OPTIMIZING FUZZY QUERIES

So far, we primarily considered ShapeQueries that had both LOCATION and PATTERN primitives mentioned for each of the ShapeSegments. However, in practice, most queries involve patterns without the location constraints (e.g., increasing followed by decreasing). We call such queries as *fuzzy ShapeQueries*, with a ShapeSegment having at least one of the start or end x locations missing as *fuzzy ShapeSegment*, and a sub-expression consisting of at least one fuzzy ShapeSegment as *fuzzy ShapeExpr*. For a *hybrid ShapeQuery*, consisting of both fuzzy and non-fuzzy ShapeExprs, ShapeSearch first computes the VisualSegments and scores corresponding to non-fuzzy ShapeExprs, and then evaluates fuzzy ShapeExprs. For ease of explanation, we assume that all ShapeExprs in the ShapeQuery are fuzzy in the rest of the section. As we will see, the results over fuzzy ShapeQueries can be extended to *hybrid ShapeQueries* by making segmentation aware of VisualSegments corresponding to non-fuzzy ShapeSegments.

In the absence of LOCATION primitives, a naive SEGMENT operator generates all possible SegmentedVizs with different combinations of VisualSegments, followed by the SCORE operator scoring all SegmentedVizs, and picking the one with the maximum score. However, exhaustive generation and scoring of all SegmentedVizs becomes expensive as the number of points in the visualization increases. For example, a simple fuzzy ShapeQuery $[p = up][p = down][p = up]$ on a visualization with 100 points can result in 10^4 possible SegmentedVizs. More generally, for a ShapeQuery consisting of k fuzzy ShapeExprs with $(k - 1)$ CONCAT operators between them, the exhaustive approach creates $(n^{(k-1)})$ SegmentedVizs, where n is the number of points in the visualization. Even a candidate visualization with a moderate number

of points can have an extremely large number of SegmentedVizs, evaluating all of which interactively is impossible. We state this problem formally:

Problem 2 (Fuzzy Segmentation). *Given a fuzzy ShapeQuery with $(k-1)$ CONCAT operators (i.e., k ShapeExpr) and a candidate visualization with n points, find k VisualSegments such that the score of the ShapeQuery is maximum.*

Our goal is to optimize the query processing for Problem 2 by minimizing the number of SegmentedVizs that we consider for scoring a fuzzy ShapeQuery. Since the ShapeExpr between two CONCAT operators can be efficiently scored over a single VisualSegment—operators other than CONCAT do not lead to segmentation—for ease of explanation we consider the intermediate ShapeExpr as one unit for the rest of the discussion.

6.1 Optimal Approach

As discussed earlier, the exhaustive approach examines all possible ways to segment a visualization, and is thus extremely slow even for a moderate number of points in the visualizations and number of ShapeExprs in the ShapeQuery. We observe that scores over smaller segments of the visualization can be reused for scoring the longer segments of the visualizations, instead of re-generating and re-scoring the smaller segments many times. Formally,

Theorem 6.1 (OPTIMAL SUBSTRUCTURE). *The optimal segmentation score (OPT) for k ShapeExprs over points 1 to n can be constructed from the optimal segmentation of k' and $(k-k')$ ShapeExprs over points 1 to n' and n' to n for some $0 \leq k' \leq k$ and $1 \leq n' \leq n$.*

In simple words, the above theorem states that the optimal segmentation for a sequence of patterns on a visualization can be constructed from optimal segmentations of subsequences of patterns over smaller regions of the visualization.

Proof: We prove the above property by contradiction. Let $OPT(1, i, [1 : j])$ be the score for the optimal segmentation over the first i values of the visualization on fitting 1 to j ShapeExprs. Assume a configuration where the scores over smaller regions of the visualization are sub-optimal, i.e., $sc(1, n', [1 : k']) < OPT(1, n', [1 : k'])$, or $sc(n', n, [k' : k]) < OPT(n', n, [k' : k])$; then on applying CONCAT between the two ShapeExprs, $sc(1, k, [1 : n]) = \frac{sc(1, k', [1 : n']) + sc(n', n, [k' : k])}{k} < \frac{OPT(1, n', [1 : k']) + OPT(n', n, [k' : k])}{k} < OPT(1, n, [1 : k])$. Therefore, scores of ShapeExprs over smaller regions of the visualization must be optimal. ■

Based on the above theorem, we jointly perform the segmentation and scoring of candidate visualizations, using a dynamic programming (DP) algorithm that implements the following recurrence:

ShapeSearch first calculates the scores for individual ShapeSegments (e.g., a , b , c , and d in $a \otimes (b \oplus (c \otimes d))$) at each of the leaf nodes. Next, it computes scores at the intermediate nodes in a bottom-up fashion, by concatenating ShapeExprs (ShapeSegments if leaf nodes) over all possible break points from the left and right children nodes, ignoring concatenated ShapeExprs that do not exist in the ShapeQuery. For example, at node 4 in Figure 7, ShapeSearch computes the scores of two-segment ShapeExprs that exist in the ShapeQuery: a , b , $a \otimes b$, $a \otimes c$, $a \otimes c$, $c \otimes d$, and $b \oplus (c \otimes d)$, formed by combining 1-segment ShapeSegments from nodes 1 and 2. At a given node, there can be duplicate ShapeExprs: for example, at node 5, $a \otimes b$ can be computed from 1) a from node 3 and b from node 4, 2) $a \otimes b$ from node 3 and b from node 4, and 3) a from node 3 and $a \otimes b$ from node 4. In such a scenario, we take the ShapeExpr with the maximum score, according to the *Closure*. This procedure is repeated until the root node of the SegmentTree, where the score of ShapeExpr corresponding to ShapeQuery is the final score.

Theorem 6.3. *Under the Closure assumption, the SegmentTree algorithm is optimal with a time complexity of $O(nk^4)$ (i.e., linear in the number of points in the visualizations).*

Proof: We prove the above theorem via induction. For a single node SegmentTree and a ShapeQuery with a single ShapeExpr, it's clear that the algorithm is optimal since there is only one VisualSegment. Next, we consider an intermediate node 5 in Figure 7, and prove that if ShapeExprs in the left child node (node 3) and the right child node (node 4) are optimal, then the computed score for a combined ShapeExpr, say $(a \otimes b)$ in node 5 is also optimal. From the Closure, the break point for $a \otimes b$ must be a subset of the break points in nodes 3 and 4. While combining, the algorithm considers all possible break points from 3 and 4, and selects the break points where the score for $a \otimes b$ is maximum. Therefore, the computed score for $a \otimes b$ must be optimal, if we assume Closure. ■

Time Complexity. Assuming there are n leaf nodes in the SegmentTree for every pair of adjacent points (the lowest possible granularity) in the visualization, there will be a total of $2n$ nodes in the tree. Moreover, for a ShapeQuery with $k-1$ CONCAT operators, there are k^2 possible ShapeExprs. And, at each intermediate node in the SegmentTree, there can be a maximum of k^4 concatenation operations (from the cross product of the k^2 ShapeExprs from the left and right node each). Therefore, the time complexity of the SegmentTree algorithm is $O(nk^4)$, which is linear in the number of points in the visualizations. The k^4 factor is acceptable since the number of ShapeExprs in the ShapeQuery is often very small. Moreover, in practice, not all combinations of ShapeExprs result in a valid ShapeExpr in a ShapeQuery, and therefore the actual number of concatenations are often fewer than k^4 .

Table 7: Bounds on scores for different patterns based on scores at a given level i in the SegmentTree

Pattern	Max possible Score	Min possible Score
<i>up</i>	max across all level i nodes	min across all level i nodes
<i>down</i>	max across all level i nodes	min across all level i nodes
<i>flat</i>	max across all level i nodes if all $\theta > 0$ or all $\theta < 0$; otherwise 1	min across all level i nodes
$\theta = x$	max across all level i nodes if all $\theta > x$ or $\theta < x$; otherwise 1	min across all level i nodes

6.3 Two Stage Collective Pruning

Even though the SegmentTree algorithm provides a significant speed-up, the overall query processing time can still be large when the number of visualizations to explore is large. To further improve the performance, we apply a two-stage optimization that identifies and prunes visualizations that are guaranteed to be not in top k . We first describe a key observation used to prune visualizations in the second stage.

Theorem 6.4 (Segment Score Boundedness). *The final score, sc_0 , of a ShapeSegment at the root node (level 0) is bounded between the maximum (sc_i^{max}) and minimum scores (sc_i^{min}) of the ShapeSegment at any given level i in the SegmentTree as defined in Table 7.*

The key idea behind the theorem is that, a pattern or trend, p , over a VisualSegment v cannot be more prominent (i.e., have a higher score) or less prominent than p over all smaller regions in v when considered individually, i.e., there should be at least one smaller region in v where p is more prominent, and one where p is less prominent than over v .

Proof (sketch): In order to prove formally, it is sufficient to show the maximum score of a ShapeSegment decreases, and the minimum scores increases monotonically as we move up the levels of the SegmentTree. We first focus on a ShapeSegment with *up* pattern, and show that the maximum score of such a ShapeSegment at a given level is non-increasing as we move up the tree. Let sc_i^{max-} be the second highest score of a ShapeSegment S at level i , and θ_i^{max} and θ_i^{max-} be the slopes of the line segments over the VisualSegments corresponding to the highest and the second highest scores respectively. Additionally, we consider a worst-case scenario where the two VisualSegments have the same parent in the SegmentTree. Let θ^P be the slope of the line segment over the VisualSegment corresponding to the parent node. Then, by the law of triangle: $\theta_i^{max-} \leq \theta^P \leq \theta_i^{max}$ and $\theta_{i-1}^{max} = \theta^P$. From Section 5.2, we know that the score of pattern *up* decreases monotonically with the decrease in slope, and therefore maximum score of the ShapeSegment is non-increasing for *up* as we move up the tree. On similar lines, we can prove that the maximum score of *down* decreases, as well as minimum scores of both *up* and *down* increases monotonically on moving up the tree. This also holds for the pattern type $\theta = x$ if slopes of all line segments at a given level lie on the same side (i.e., $\theta_i > x$ or $\theta_i < x$), otherwise we set the maximum score to 1 (the maximum possible value). Thus, the final score (sc_0)

is bounded between the maximum (sc_i^{max}) and minimum (sc_i^{min}) scores at level i , as defined in Table 7. ■

Additionally, from Property 5.1, we know that the scores of operators are bounded between the minimum and maximum scores of ShapeSegments, which implies that scores of ShapeExprs are also bounded between the minimum and maximum scores of the ShapeSegments. Thus, we can derive upper and lower bounds on the overall score of a ShapeQuery at a given level i using the following three steps: 1) Compute the maximum and minimum scores for each of ShapeSegment involved in the ShapeQuery. 2) Compute the maximum and minimum scores for each ShapeExpr between two CONCAT operators using the maximum or minimum scores of the ShapeSegments. 3) Apply CONCAT on the maximum and minimum scores of the ShapeExpr to get the upper and lower bound on the final score. Nevertheless, bounds on the overall score can be loose at the leaf nodes since these nodes consist of small line segments with varying slopes. As such, we precede the pruning stage with another light-weight sampling stage to come up with better lower bounds on top k scores. We, now, describe the two stages.

Stage 1: Identifying lower bounds. We randomly sample a small set of visualizations, and for each sampled visualization, we perform a DP-based scoring on a subset of points distributed uniformly across the visualization. The lowest score among the top- k visualizations (in the sampled collection) gives a lower bound on the overall top- k visualizations.

Stage 2: Refining and pruning. In the second stage, instead of processing each visualization completely in one go, we process visualizations in rounds. In each round, we process a few levels of SegmentTree for all of the visualizations simultaneously, and incrementally refine the upper and lower bounds on their scores. Before moving on to the upper levels, we prune the visualizations that have their upper bounds lower than the current top- k lower bound score.

Overall, the two stage collective pruning helps avoid processing until the root node for the majority of visualizations in the collection, and is particularly effective when the user is looking for visualizations with rare (e.g., needle-in-the-haystack) patterns. As potential future work, we believe more sophisticated techniques leveraging sampling and simulated annealing can further help in pruning.

7 USER STUDY

We conducted a user study to evaluate the utility of ShapeSearch (relative to visual query systems [8, 29, 44]) on its ability to effectively support pattern matching tasks in trend-lines. We also wanted to understand which tasks are easier to express in each of the specification mechanisms: sketch, natural language, and regular expression. We first describe the user study methodology, followed by our key findings from the study. In the next section, we present a case study

Table 8: Overall Results

Tool	Average Accuracy	Average Time
VQS (only sketch)	71%	184s
ShapeSearch* (NL or regex)	88%	105s

Table 9: Preferences

Interface	Preference
VQS (sketch)	1/12
ShapeSearch* (NL and regex)	4/12
ShapeSearch (sketch, NL, and regex together)	7/12

with bioinformatics researchers working on genomics data for a more open-ended evaluation of the tool.

7.1 User Study Methodology

Participants. We recruited 12 participants (7 male, 5 female) with varying degrees of expertise in data analytics via flyers and mass-emails. Out of the 12 participants, 7 were graduate students, 3 were undergraduate students, 1 was a post-doctorate scholar, and 1 was an university employee. While all the participants reported working weekly with data or visualizations (e.g., using excel), 9 out of the 12 participants had prior experience in programming languages (e.g., R, Python, Pandas, and MATLAB), and 5 participants had used SQL before.

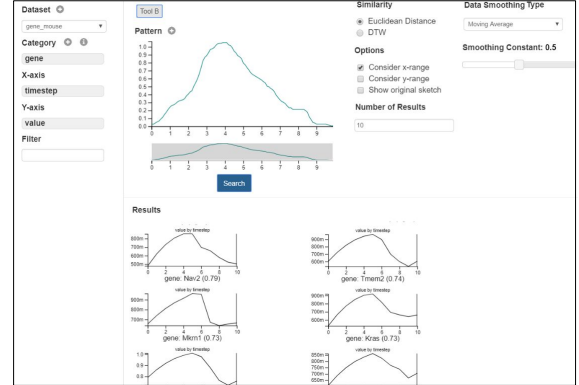


Figure 8: Baseline Interface

Baseline. For the purposes of our study, we explicitly wanted to do a head-to-head qualitative and quantitative comparison of ShapeSearch tool, primarily the natural language and regular expression interfaces, with visual query systems that support a sketch-based querying mechanism for searching for shapes. Thus, we developed a baseline tool, depicted in Figure 8, that replicated the capabilities of these systems with a styling scheme identical to the ShapeSearch tool to control for external factors. The baseline tool allows users to specify the x -axis attribute, y -axis attribute, and filters; sketch pattern on a canvas, choose the shape matching measure; zoom in and out of the visualization to focus on specific regions of the visualization; and apply smoothing to match visualizations at varying granularities. On the other hand, we disabled the sketching capability in ShapeSearch for a

Table 10: Pattern Matching Tasks

Tasks	Description (Example Queries)	Symbol
Exact Trend Matching	Find shapes similar to a specific shape (cities with weather patterns similar to that of NY, stock trends similar to Google's)	ET
Sequence Matching	Find shapes with similar trend changes over time (cities with following temperature trends over time: rise, flat, and fall, stocks with decreasing and then rising trends)	SQ
Sub-pattern matching	Find frequently occurring sub-pattern (or motif) (stocks that depicted a common sub-pattern found in stocks of Google and Microsoft, cities with 2 peaks in temperature over the year)	SP
Width specific matching	Find shapes occurring over a specific window (cities with maximum rise or fall in temperature over 3 months, peaks with a width of 4 months)	WS
Multiple X or Y constraints	Find shapes with patterns over multiple disjoint regions of the visualization. (stocks with prices rising in a range of 30 to 60 in march, then falling in the same range over the next month)	MXY
Trend Characterization	Summarizing common trends (e.g., find cities with typical weather patterns, stock with typical price patterns)	TC
Complex Shape Matching	Find shapes involving trends along specific directions, and occurring over varying duration (stocks with head and shoulder pattern, cup-shaped patterns, W-shaped patterns)	CS

fairer comparison. ShapeSearch* denotes ShapeSearch with only NL- and regex-based querying mechanisms.

Dataset and Tasks. Based on the case studies that served domains we discussed in Introduction, as well as drawing on time series and pattern recognition papers from the data mining [13, 18, 32, 38, 48] and visualization community [8, 10, 11, 29, 44]; we identified seven subcategories of pattern matching tasks, as depicted in Table 10. We designed these tasks on two real-world datasets: the Weather and the Dow Jones stock datasets from the UCI repository [5] that participants could easily understand and relate to. Together the seven tasks touched upon both exploratory search as well as direct / specific pattern-based data exploration, which helped us better gauge the effectiveness of individual interfaces.

Study Protocol. We conducted the user study using a within-subjects study design, in three phases. First, participants were provided a 15-minute tutorial-cum practice session per tool to get familiarized before performing the tasks. Next, we asked the participants to perform the aforementioned tasks with the orders of the two tools and tasks randomized to reduce any order effects. Participants had to answer between 3 to 5 visualizations that were most relevant to the task. Finally, we asked the participants to complete a survey and answer open-ended questions that measured 1) their satisfaction levels, and preferences among the three interfaces for each of the task, 2) strengths and weaknesses of the interfaces; and 3) usefulness of the tools in participants' daily work.

Ground Truth. For each of the tasks, three of the authors assigned a score in a range of 0 (worst match) to 5 (best match) for each of the candidate visualizations for the tasks. We took the average of the three scores to rate the participants answers.

Metrics. From data that we recorded during the study, we collected the following metrics: 1) *Task completion time*: the time taken by the participant to provide the their answers for the task. 2) *Task accuracy*: (sum of the scores of the visualizations answered by the participant)*100 / (sum of the scores of the visualizations in the ground-truth). 3) *Preferences* among the three interfaces, and between the tools for individual

tasks as well as overall. 4) *Satisfaction level* with the two tools on a 5-point Likert scale. In addition, we also analyzed open-ended subjective answers given by participants during the interview sessions.

7.2 Key Findings

Now, we describe the key findings from our analysis of the metrics collected during the study.

How accurate were participants' answers using ShapeSearch and VQS? How long did it take them to finish the tasks? As depicted in Table 8, ShapeSearch* helps participants achieve higher accuracy (87%) over VQSs (70%) in about 40% less time, a significant improvement both in accuracy and task completion times. While the visual query system involves less reasoning during the query synthesis, it often leads to significantly more manual browsing of candidate visualizations for identifying the desired ones. ShapeSearch, on the other hand, is able to accept more fine-grained user input, and rank relevant visualizations higher, enabling participants to retrieve more accurate answers with less effort.

How ShapeSearch and VQS compare on individual pattern-matching tasks? In order to better understand the differences between the tools, we analyzed accuracy and latency results on a per-task basis as depicted in Figure 9a and Figure 9b respectively, and compared these results with the user preferences (Figure 9c) for individual querying mechanism (collected via survey forms and interview questions). Overall, we found that the accuracy and the task completion times are closely related with the expressivity of the tools. We summarize our findings below.

More number of participants (9/12) preferred sketch-based querying interface compared to ShapeSearch (7/12) for precise pattern matching tasks that involved finding visualizations that were exactly similar to a given visualization. Moreover, participants gave more accurate answers in relatively less time while using sketch-based querying. Participants (4/12) who preferred both mentioned they would use sketch if they want to search for visualizations that had similar values to

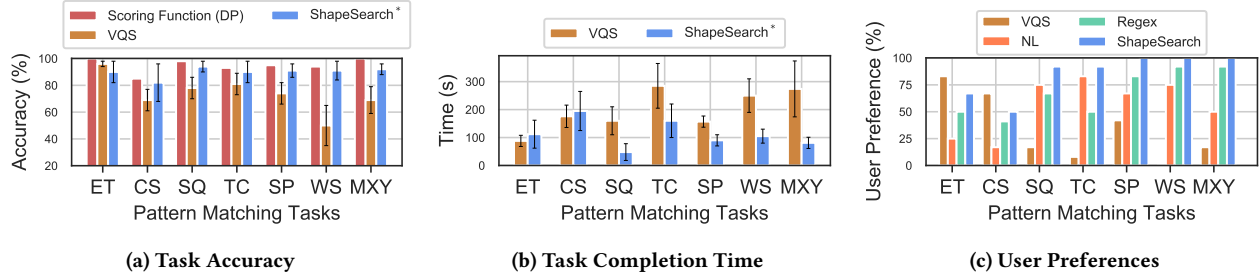


Figure 9: User Study Results

the given visualization, but would use either NL or Regex if they want to search for high-level changes in trends over time.

While searching for complex shapes (e.g., stocks with double top pattern), more participants (7/12) tend to prefer sketch-based querying, and took less time to complete their tasks compared to ShapeSearch (6/12). However participants had more accurate answers when using ShapeSearch. Participants believed it is less effort to sketch and modify complex shapes on the canvas and select dynamic time warping (DTW) for finding similar shapes, compared to writing a regex. However, ShapeSearch resulted in higher accuracy because the scoring methodology used in ShapeSearch is better at abstracting trends, and more robust to random fluctuations in sequence values than the DTW measure which compares and aligns visualizations solely based on values.

Majority of the participants (11/12) preferred ShapeSearch for searching visualizations with a sequence or a subsequence of patterns, and provided more accurate answers in less time. Since visual query systems are based on precise sketch matching, users have to draw multiple sketches for a given sequence or subsequence to find all possible instances. ShapeSearch, on the other, is more effective at automatically finding a variety of shapes that satisfy the same sequence or subsequence of patterns.

For tasks involving multiple constraints along the X and Y axes, or the width of patterns, a large majority of the participants preferred ShapeSearch, and provided more accurate results in less time. This is because ShapeSearch supports a rich set of primitives for users to add multiple constraints on the patterns, including searching patterns over multiple disjoint regions. While the users could zoom into a specific region of the visualization and sketch their desired patterns in the visual query system, these capabilities were not sufficient to precisely specify all constraints at the same time. We believe effectively implementing primitives supported by ShapeSearch using visual widgets, and providing effective coordination between the widgets and the canvas is a challenging task, and is an interesting future work.

Overall, when we asked participants which tool they would prefer for pattern matching tasks in their workflow, 11 out of

12 participants preferred ShapeSearch (with three interfaces integrated together) over visual query systems. Only 1 participant considered visual query systems sufficient for her data analysis work, while 4 participants believed natural and regex together without sketch can be sufficient. Participant P2 said “Almost always, I will go with Tool B [ShapeSearch*]. I know exactly what I am searching [for] and what the tool is going to do, it is much more concise, I feel more confident in expressing my query pattern”. On a 5-point Likert scale ranging from strongly disagree (1) to strongly agree (5), participants rated visual query systems 2.8 and ShapeSearch 4.2 when asked about how effectively and flexibly these tools helped them express their intended patterns.

Which querying mechanism is more useful between NL and regex? Out of 11 participants who preferred ShapeSearch over visual query systems, 7 said they would opt for regex over natural language and sketch, if they had to choose one. This was surprising given 5 of these participants had no prior experience with regular expressions-like languages. Participant P8 said “the concept for visual regex by itself is very powerful, could be helpful for most cases in general”. Participant p4 said “Regex was very friendly to use, very powerful for a large number of usecases”. On the other hand, participant P1 who preferred natural language over regex said, “Natural language and drawing [sketching-based querying] are good [sufficient] for most of the patterns, once or twice [rarely] I will search for complicated patterns with constraints, but I can then first use natural language and then fill the missing fields in the [form-based correction] panel below...”. On a 5-point Likert scale ranging from strongly disagree (1) to strongly agree (5), participants gave a score of 3.9 when asked how effective ShapeSearch was in understanding and parsing their natural language queries. And when asked how easy it was to learn and apply regular expression, they gave a rating of 4.2.

How effective is line-segments-based shape matching?

When asked about the effectiveness of using line-segments for approximating and matching trendlines, the average response was positive with a rating of 3.9 on a scale of 5. Participant 4 said “Green lines [line-segments fitted over the visualization in ShapeSearch] are good, they make me more confident, help me understand visualizations especially [the]

noisy ones without me having to spend too much time parsing signals. I can also see how my [query] pattern was fitted over the visualization ...”.

How can ShapeSearch be improved? Participants suggested several improvements to make ShapeSearch more useful in their workflows. A large number of participants wanted ShapeSearch to support more mathematical patterns by default like concave, convex, exponential, or statistical measures such as entropy. For line-segment based approximations, participants suggested we use different colors for lines that correspond to different patterns (ShapeSegments) in the ShapeQuery. Moreover, syntax for regex can be made simpler by removing square brackets, supporting better symbols for primitives and operators, and supporting more real time regex validation and auto-correction. Finally, a few participants suggested that we should recommend queries and visualization based on learning from historical queries. .

7.3 Effectiveness of Scoring Functions

We evaluated the effectiveness of ShapeSearch scoring functions compared to DTW- and Euclidean-based (both supported options in VQS) shape similarity measures on the ground-truth results. Since the answers can vary depending on the drawn trendline (sketch) and settings (e.g., smoothing) of the VQSs, for Euclidean and DTW, we used the answers provided by participants based on their judgment. Moreover, between DTW and Euclidean, participants were free to choose the option that they felt was more appropriate and relevant to the task. For ShapeSearch scoring functions, we used the DP-based optimal algorithm for ranking visualizations. Note that during the study, we used SegmentTree-based algorithm for ranking visualizations (results depicted via blue bars in Figure 9a), since the optimal algorithm is too slow (discussed in more detail in Section 9). As depicted in Figure 9a (red bar) ShapeSearch scoring functions have an accuracy of over 89% accuracy for about 6 out of the 7 tasks. VQSs, as discussed earlier, have a comparatively lower accuracy of 71%. On complex shape matching tasks, ShapeSearch scoring functions have a relatively less accuracy of 81% than over other tasks, but is still better than the average accuracy of responses provided by the participants while using VQSs.

8 CASE STUDY : GENOMICS

Here, we present a case study with bioinformatics researchers working on genomics data for a more open-ended evaluation of the tool. We invited two bioinformatics researchers R1 (a 5th year graduate student) and R2 (a 2nd year graduate student) at a major university. Both researchers perform pattern analysis on genomic data on a daily basis using a combination of spreadsheets and scripting languages such as R. We asked participants to send us a popular dataset they often analyze prior to the study (mouse gene data [7]) and ensured

that ShapeSearch operated on their dataset as expected. We summarize our findings below.

We started the study with a 15 minute introduction and a demo of the ShapeSearch tool on the Weather data set that we had also used for the user-study, and asked participants to perform a few pattern matching tasks to help them familiarize themselves with the tool, as well as to ensure that they understood the functionalities of the tool.

Next, we encouraged participants to use ShapeSearch to explore their data. Since we were interested in seeing if they could create queries that reveal previously unknown insights, we requested our participants to think aloud, explain the kind of queries they were constructing, whether the results confirmed some already known fact, and how they currently performed such exploration using existing tools. This also helped us ensure that their mental model was matching with what the queries actually expressed. Each session lasted for about 75 minutes.

8.1 Findings and Takeaways

I. *Both the participants were able to grasp the functionalities of the system after a 15 minute introduction and demo session without much difficulty.* They answered questions that were asked to test their understanding with almost 100% accuracy. There were positive reactions from the participants during the introduction and demo like “(R1) *oh, this feature [searching using combinations of patterns such as up and down] is cool, ... something that we frequently do*”, “(R2) *I like that you can change your patterns [queries] that easily, and see the results in no time...*”. Both participants concurred that ShapeSearch could be a valuable tool in a biologist’s workflow, and can help perform faster pattern-based data exploration, compared to current scripting R or spreadsheet approaches .

II. *Using succinct queries, participants could interactively explore a large number of gene groups, depicting a variety of gene expression patterns.* Both R1 and R2 were able to query for genes with differential expressions over time. During the initial part of the study, R1 issued natural language queries to search for genes that suddenly start expressing themselves as some point, and then gradually stop expressing. These expression changes signify an effect of external stimulus such as a chemical or a treatment. Before the treatment, the affected genes are stable with low expressions, immediately after the treatment they suddenly get expressed, and then as the effect of treatment subsides, the expression reduces gradually. Thereafter, R1 was interested in understanding the variations in expression rates. For instance, expressions in certain groups of genes rise and fall much faster, while in others expression changes are gradual. In order to search for these patterns, she interactively adjusted the width of patterns in her queries. R1 could also see groups of genes that show similar changes in expression over time, indicating they regulated similar cell mechanisms.

III. ShapeSearch *helped participants validate their hypotheses, and make new discoveries*. Related to his area of research, R2 used regex to explore a group of genes that increase with a slope of 45° until a certain point, and then remain high and flat, as well as the ones that depicted the inverse behavior (ones that start high and then gradually reduce their expression and remain low and flat). Such patterns in expressions are often symbolic of permanent changes (e.g., due to aging) in cell mechanisms and are often seen among genes in stem cells. During early stages (known as self-renewal) stem cells repeatedly generate themselves (indicated by higher expression), and then gradually differentiate into other cell types (e.g., muscle cells), depicted by low and stable expression values. While exploring these patterns, R2 discovered two genes, *gbx2* and *klf5*, in the results panel, that had similar expression patterns, and mentioned that the two genes indeed had similar functionality at any point in time and are actively researched by scientists working in stem cells. Next to these two genes, he saw another gene *spry4* with almost similar expression, and hypothesized that the similarity in shape indicates that *spry4* possibly had similar functionalities to *gbx2* and *klf5*, something that not many researchers know, and could lead to interesting discoveries if true.

IV. ShapeSearch *helped participants find genes with unexpected or outlier behaviors*. During the end of her study, R1 mentioned that it is rare to see a gene with two peaks in their expressions within a short window. However, on searching for this pattern via natural language, she found a gene named “*pvt1*” having two peaks within a short time duration of 10 time points, something that she found surprising and strange. She thought it might be either because of some preprocessing error, or some rare activity happening in the cell. Surprised by this result, she went ahead and searched for other patterns that she thought were outliers (e.g., three peaks, always increasing).

Overall, comparing between NL and regex, R1 said she could express most of her queries using natural language, and would use regex only when the pattern is too long, and involves multiple constraints. R2, on the other hand, said he would use regex in all scenarios. He believed regex was not significantly difficult to learn, and helped him feel more in control and confident about what he was expressing, and whether the system was correctly inferring and executing his issued queries.

V. *Participants faced a few challenges during exploration*. They wanted to switch back and forth between queries, so that they do not have to remember and reissue their previous queries. In addition to better presentation of the fitted lines (e.g., coloring), they wanted to understand in more detail how the scores were computed, and if they could tweak the scoring according to their needs using visual widgets.

9 PERFORMANCE EVALUATION

In this section, we evaluate the performance of ShapeSearch execution engine on real datasets, focusing on overall run-time and accuracy. We also vary the characteristics of ShapeQueries to assess the impact of different factors on performance.

Algorithms. We compare the following algorithms: (i) the dynamic programming-based (DP) optimal algorithm from Section 6.1, (ii) the SegmentTree-based pattern-aware scoring algorithm from Section 6.2, (iii) the SegmentTree algorithm with push-down optimizations from Section 5.4, (iv) the SegmentTree algorithm with both push-down and two-stage collective pruning from Section 6.3, (v) a *greedy* segmentation-based approach, where we start with equal-sized VisualSegments, and incrementally extend or shrink (by half) the lengths of VisualSegments, until there is no improvement in the overall score. For example, if a SegmentViz has two VisualSegment from 1 to 10 and 10 to 20 at round i , then in round $(i + 1)$, we consider SegmentedVizs with following VisualSegments boundaries: 1) 1 to 5 and 5 to 20, and 2) 1 to 15 and 15 to 20, and select the one with the maximum score, (vi) dynamic time warping (DTW) [36], a state-of-the-art shape matching approach. During our user study, we had evaluated the effectiveness of DTW in capturing various shape-matching tasks. Here, our goal is to compare its efficiency compared to ShapeSearch algorithms, and accuracy with respect to our proposed scoring functions discussed in Section 5.2.

Datasets and Setup. As summarized in Table 11, we evaluate ShapeSearch on five publicly available and *diverse* real-world datasets: Weather, Worms, 50 Words, Haptics from the UCI repository [5], and Real Estate dataset from zillow.com [6]— each dataset contains trendlines with a mix of shapes, and differ from each other in terms of number of trendlines as well as their length. Real Estate dataset, unlike the other dataset, has multiple y values per x coordinate, and hence required aggregation (*avg*) before shape-matching. All experiments were conducted on a 64-bit Linux server with 16 2.40GHz Intel Xeon E5-2630 v3 8-core processors and 128GB of 1600 MHz DDR3 main memory. Datasets were stored in memory, and we ran six trials for each query on each dataset, ignoring the results from the first trial and taking the average across the rest of the five trials.

9.1 Overall Run-time and Accuracy

We first compare the performance of algorithms on *fuzzy* queries, for which ShapeSearch explores a large number of SegmentedVizs for every candidate visualization. The performance of ShapeSearch algorithms on non-fuzzy queries is similar, since each candidate visualization segments into only one SegmentedViz. Non-fuzzy queries, however, are still amenable to push-down optimizations, which we discuss later in the section.

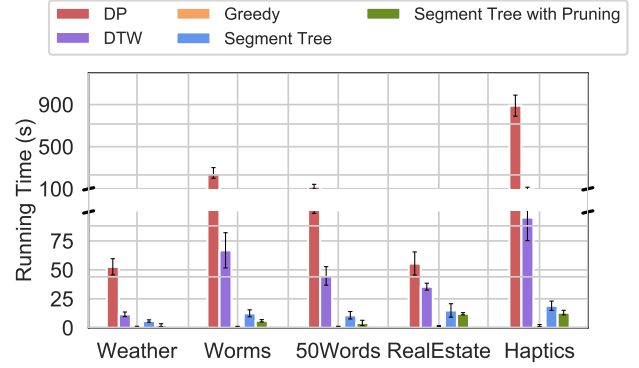
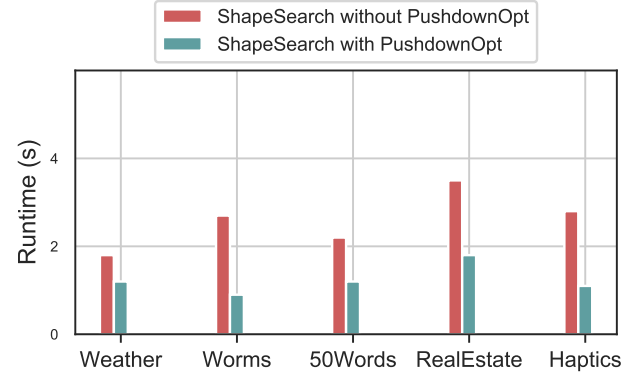
Table 11: Real-world Datasets and Query Characteristics

Name	Visualizations	Length	Fuzzy Queries	Non-Fuzzy Queries
Weather	144	366	$(\theta = 45^\circ \otimes d \otimes u \otimes d), ((u \otimes d) \otimes f \otimes u \otimes d), (f \otimes u \otimes d \otimes f)$	$([p\{down\}, x.s = 1, x.e = 4] \otimes [p\{up\}, x.s = 4, x.e = 10] \otimes [p\{down\}, x.s = 10, x.e = 12])$
Worms	258	900	$(d \otimes (\theta = 45^\circ \otimes \theta = -20^\circ) \otimes f), (d \otimes \theta = 45^\circ \otimes d), (u \otimes d \otimes u)$	$[p\{down\}, x.s = 50, x.e = 100]$
50 Words	905	270	$(d \otimes (u \otimes (f \otimes d))), (f \otimes u \otimes d \otimes f), ((u \otimes d) \otimes (u \otimes d) \otimes f)$	$[p\{down\}, x.s = 200, x.e = 400] \otimes [p\{up\}, x.s = 800, x.e = 850]$
Real Estate	1777	138	$(f \otimes d \otimes u \otimes f), (u \otimes d \otimes u \otimes f), (u \otimes f \otimes (\theta = 45^\circ \otimes \theta = 60^\circ) \otimes (u \otimes d)))$	$[p\{down\}, x.s = 1, x.e = 20] \otimes [p\{up\}, x.s = 20, x.e = 60] \otimes [p\{down\}, x.s = 60, x.e = 138]$
Haptics	463	1092	$(u \otimes d \otimes f \otimes u), (d \otimes u \otimes d \otimes f)$	$[p\{up\}, x.s = 60, x.e = 80]$

Table 11 depicts the fuzzy ShapeQueries that we issued over each of the five real-world datasets. We selected fuzzy ShapeQueries that had atleast 20 visualizations with score > 0 , which helped ensure that the issued ShapeQueries were relevant to and ended up matching visualizations in the dataset. Using the results from the DP-based optimal algorithm as ground-truth, we define the accuracy as the number of visualizations picked by the algorithm that are also present in the top k visualizations selected by DP.

Figure 10 depicts the runtime of algorithms, while Figure 12 depicts the accuracy results over top- k visualizations (with k varying from 2 to 20). Annotations in Figure 12 depict the average deviation in % of the score of k th visualization that an algorithm selects with respect to the score of the k th optimal visualization, indicating how off the shapes of selected visualizations are from optimal ones. We observe that SegmentTree provides a 2X to 40X improvement in runtime with an average accuracy of $> 85\%$ compared to DP. The runtime for DP is quadratic in the number of points in the visualization, and can take 10s of seconds even for visualizations with only a few hundred points. SegmentTree, on the other hand, is extremely fast even over visualizations with more than 1000 points (since its runtime varies linearly with the number of points), and selects visualizations that are almost similar to that of DP. We note that the accuracy of SegmentTree improves as the number of output visualizations increases, and is never off by more than 2 visualizations or have more than $> 12\%$ deviation in scores when we look at top 20 visualizations. SegmentTree with Pruning further provides a speed-up of 10-30% by identifying and pruning low utility visualizations that do not have patterns specified in the ShapeQueries.

The greedy algorithm, not surprisingly, has the least runtime ($< 2s$) among all, but incurs a much more severe penalty in accuracy ($< 30\%$), selecting visualizations that are less similar to the optimal ones. This is because the greedy algorithm tries only a few SegmentedVizs after which it hits a local optimum, and stops. DTW’s runtime is better than that of DP (by a factor k , the number of ShapeSegments in the ShapeQuery), but worse by up to 10X compared to SegmentTree-based algorithm, and has a moderate (40 – 60%)


Figure 10: Average running time over five datasets (error bars indicate the maximum and minimum runtimes)

Figure 11: Average running time before and after push-down optimizations on non-fuzzy queries.

accuracy when compared with the ground-truth visualizations selected using ShapeSearch scoring methodology. The moderate accuracy is primarily because of the fact that DTW measure is poor at capturing blurry trends in the visualizations. Together with the user study findings, the performance results demonstrate that *compared to DTW, ShapeSearch is more effective, efficient, and preferred for searching for shapes in trendlines.*

Impact of Push-Down Optimizations. Next, we issue non-fuzzy queries (one query on each of the dataset [4]) to evaluate the impact of pushdown optimizations. Figure 11 depicts the runtimes for ShapeSearch (note that all ShapeSearch algorithms behave similar for non-fuzzy queries) with and without push-down optimizations. We observe that non-fuzzy queries execute very quickly ($< 4s$ for over 1000 visualizations with more than 1000 points each), but pushdown optimizations help in further reduction of runtime in proportion to the selectivity of the *LOCATION* primitives in the query. For example, for ShapeQuery $[p\{up\}, x.s = 60, x.e = 80]$ on the haptics dataset, pushdown optimizations help reduce the runtime from 3s to $< 1.2s$.

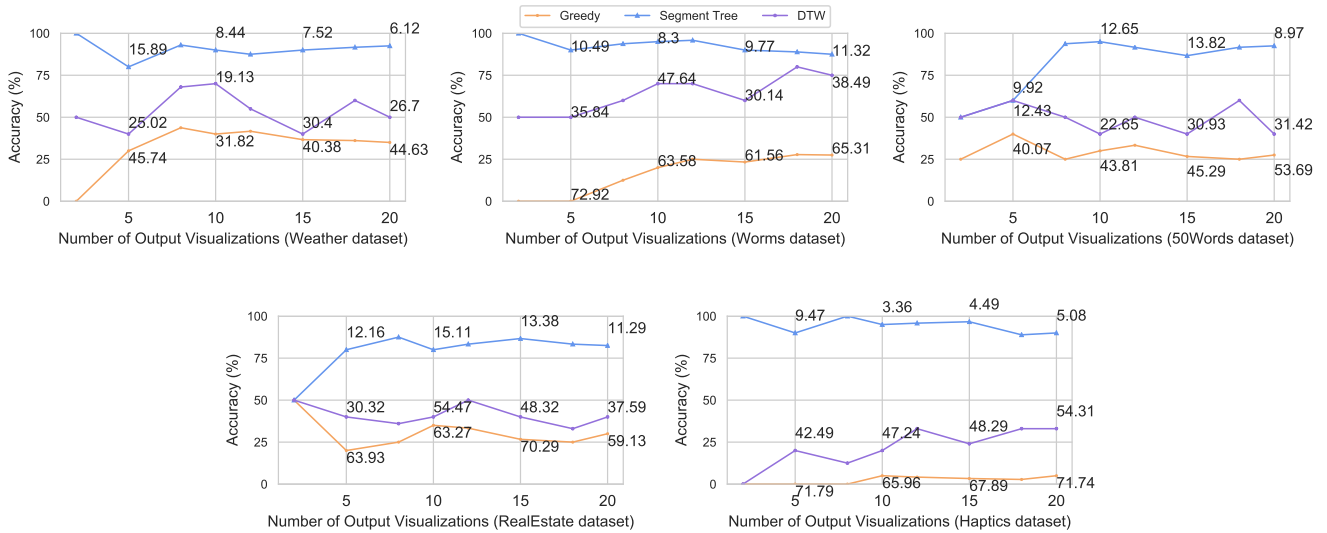


Figure 12: Accuracy over five real datasets with varying number of output visualizations. Annotations denote the average deviation (in %) of the score of k th visualization chosen by algorithms with respect to the k th optimal visualization.

9.2 Varying Characteristics of ShapeSearch Queries

We evaluated the efficacy of our SegmentTree-based optimizations with respect to three different characteristics of ShapeQueries, as discussed below.

Impact of number of data points. For varying data points, we selected the first 50, 100, 200, ..., 900 points from each visualization in the Worm dataset to create ten sub-datasets, and issued a fuzzy ShapeQuery ($u \otimes d \otimes u \otimes d$) on each of the dataset independently. Figure 13 shows the performance of algorithms as we increase the number of data points. With the increase in data points, the overall runtimes increases for all algorithms because of the increase in the number of segmentations. Nevertheless, SegmentTree shows better performance than DP after 100 data points due to the fact that the runtime for SegmentTree approach is less sensitive (linear time) to the number of data points than that of Dynamic Programming (quadratic).

Impact of number of patterns. We composed fuzzy ShapeQueries with varying number of ShapeSegments (alternating *up* and *down* patterns) and issued them over the weather dataset. We depict the results in Figure 13. As the number of ShapeSegments in the ShapeQuery grows, the overall runtimes of the algorithms also increases, with the runtimes for SegmentTree and SegmentTree with pruning growing much faster (k^4) than DP (k). However, the overall time for DP was still larger because the number of data points (366 in the weather dataset) plays a more dominant (n^2) role.

Impact of number of visualizations. We increased the number of visualizations from 100 to 1000 in the real-estate dataset with a step size of 100 and issued a fuzzy ShapeQuery ($u \otimes d \otimes u \otimes d$); the results are depicted in Figure 13. While the overall runtime for all approaches grows linearly with the number of visualizations, the gap between SegmentTree and SegmentTree with pruning grows wider. This is because more number of visualizations get pruned as the size of the collection grows larger.

10 RELATED WORK

Our work draws on prior work in time series similarity, data mining, as well as visual querying and natural language interfaces for interactive data exploration.

Time Series Similarity. There is a large number of similarity measures such as Euclidean distance, Dynamic Time Warping (DTW) [37, 41], and cross-correlation-based [33] measures that are used for comparing time-series. Unlike Euclidean distance that performs point-wise comparison, DTW and cross-correlation are considered better fits for shape matching, especially when trendlines have similar shapes, but are not aligned along the x axis (e.g., with a phase difference). To achieve scaling and translation invariances, time-series are often z -normalized before matching [16]. Most distance measures perform value-based comparisons between trendlines, and are, therefore, most effective when the trendlines being compared are from the same data set (e.g., finding nearest-neighbours for a given trendline), or when the input pattern can be precisely sketched, and translated to the domain of targeted trendlines. ShapeSearch, on the other hand,

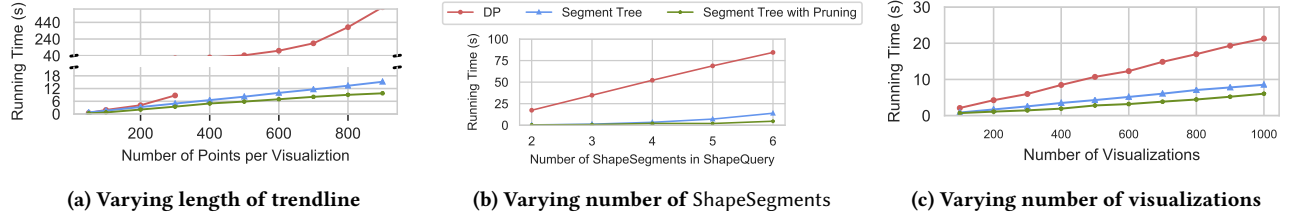


Figure 13: Runtimes on Varying Characteristics of ShapeQueries

provides *declarative* and more *expressive* querying mechanisms for searching for shapes based on atomic primitives, and their combinations. Since comparisons are not directly based on proximity of values, ShapeSearch is less affected by local distortions or outliers, and therefore better suited for *blurry* matching scenarios.

Symbolic Pattern Mining and Querying. There are a number of symbolic approaches [12, 28, 43] that discretize a time series into a sequence of symbols (or events), and use variants of string matching algorithms such as edit-distance or longest common subsequence to find similar sequences present in the input trendline. Having a fewer number of discrete symbols as opposed to continuous points also helps in making similarity search efficient. For example, Shape Definition Language (SDL) [34], like ShapeSearch, allows users to search for trendlines with specific pattern sequences via a structured keyword-based input. Like other indexing-based approaches, [20, 22, 23, 26, 43], SDL segments each time-series into fixed-length segments, and indexes them with closest matching pattern symbols in advance — trading-off flexibility and precision for efficiency. Similarly, SPIRIT [15] is a regular-expression-based tool that incorporates user-controlled constraints for mining frequent patterns in sequence databases. The major downside with this line of work (and a key distinguishing factor compared to ShapeSearch) is that the detailed information about each trendline is difficult to faithfully abstract in advance to answer all possible shape queries. Moreover, a time-series can have varying shape for different filters and aggregations, often applied on-the-fly during ad hoc data exploration (e.g., Figure 1c). Therefore, instead of representing a trendlines as a sequence of patterns, or using indexes, ShapeSearch leverages online query-aware optimizations for efficient pattern matching. Allowing real-time pattern matching over arbitrary subsets of data with varying granularity and aggregation, makes ShapeSearch more suitable for ad hoc data exploration scenarios.

Visual Querying Tools. Our work builds upon a number of visual querying tools that provide interactive specification mechanisms to search for trendlines. Query sketching tools [29, 31, 40, 44, 47] help search for shapes by taking as input the sketch of the desired shape. Most of these tools either use precise similarity measures such as Euclidean distance or DTW for shape matching, and therefore suffer from the same issues we discussed earlier. TimeSearcher [8] and

its variants let users apply soft or hard constraints on x and y range values via boxes or query envelopes, but do not support mechanisms for specifying shape primitives beyond location constraints. Similarly, there are a number of tools [17, 19, 31] that target specific shapes and outline important perceptual features for effective shape matching. However, the major difficulty with these tools is their limited query expressiveness, along with the black-box nature of query execution with each shape often having its own processing or matching steps. ShapeSearch generalizes these tools with a concise algebra, that, besides improving expressivity and composability, helps reason about query execution and potential optimizations for a wide-variety of shapes under one umbrella, making the tool scalable to larger datasets. An important and challenging future work is to develop visual specification widgets corresponding to ShapeSearch algebra primitives, that allows users to compose a large number of shape queries without overwhelming them.

Natural Language Specification. There is also a large body of work on keyword- and natural language-based interfaces for querying databases [27] and generating visualizations [14, 42]. However, since the underlying shape query algebra in ShapeSearch is different from SQL, parsing and translation strategies from existing work cannot be easily adapted. Recently, conversation-based systems such as AVA [21], and the visual data exploration language ZQL [44] have been proposed. However, these systems provide a high level framework for facilitating and automating the insight search, but consider pattern matching tasks over individual visualization as black-boxes.

11 CONCLUSION

We presented ShapeSearch, an end-to-end pattern searching system, providing expressive and flexible mechanisms for domain experts to effortlessly and efficiently search for trendline visualizations with desired shapes. We described ShapeQuery algebra that forms the core of ShapeSearch, and helps express a large variety of patterns with a minimal set of primitives and operators as well as the execution engine that enables on-the-fly and scalable pattern matching. Our general-purpose user study, case-study with genomics researchers, and the findings from the performance experiments demonstrate efficiency, effectiveness, and usability of the system. In conclusion, our work is a promising first step towards a flexible, efficient, and extensible framework

for pattern-based data exploration that caters to the needs of both expert and novice domain experts.

REFERENCES

- [1] Investopedia. <https://www.investopedia.com/terms/t/tripletop.asp>.
- [2] Law of diminishing returns. <https://bit.ly/2ONXTS5>.
- [3] Python crf-suite library (<https://github.com/albertaueyung/python-crf-named-entity-recognition>). [Online; accessed 1-Oct-2018].
- [4] Technical report. <https://goo.gl/XX2P24>.
- [5] Uci repository. <https://archive.ics.uci.edu/ml/datasets/>.
- [6] Zillow real estate data (<http://www.zillow.com/research/data/>). [Online; accessed 1-Feb-2016].
- [7] C. J. Bult, J. T. Eppig, J. A. Kadin, J. E. Richardson, J. A. Blake, and M. G. D. Group. The mouse genome database (mgd): mouse biology and model systems. *Nucleic acids research*, 36(suppl_1):D724–D728, 2008.
- [8] P. Buono, A. Aris, C. Plaisant, A. Khella, and B. Shneiderman. Interactive pattern search in time series. In *Visualization and Data Analysis 2005*, volume 5669, pages 175–187. International Society for Optics and Photonics, 2005.
- [9] E. Charniak. Statistical parsing with a context-free grammar and word statistics. *AAAI/IAAI*, 2005(598-603):18, 1997.
- [10] M. Correll and M. Gleicher. The semantics of sketch: Flexibility in visual query systems for time series data. In *Visual Analytics Science and Technology (VAST), 2016 IEEE Conference on*, pages 131–140. IEEE, 2016.
- [11] M. Correll and J. Heer. Regression by eye: Estimating trends in bivariate visualizations. In *ACM Human Factors in Computing Systems (CHI)*, 2017.
- [12] C. Faloutsos, M. Ranganathan, and Y. Manolopoulos. *Fast subsequence matching in time-series databases*, volume 23. ACM, 1994.
- [13] T.-c. Fu. A review on time series data mining. *Engineering Applications of Artificial Intelligence*, 24(1):164–181, 2011.
- [14] T. Gao, M. Dontcheva, E. Adar, Z. Liu, and K. G. Karahalios. Datatone: Managing ambiguity in natural language interfaces for data visualization. In *Proceedings of the 28th Annual ACM Symposium on User Interface Software & Technology*, pages 489–500. ACM, 2015.
- [15] M. N. Garofalakis, R. Rastogi, and K. Shim. Spirit: Sequential pattern mining with regular expression constraints. In *VLDB*, volume 99, pages 7–10, 1999.
- [16] D. Q. Goldin and P. C. Kanellakis. On similarity queries for time-series data: constraint specification and implementation. In *International Conference on Principles and Practice of Constraint Programming*, pages 137–153. Springer, 1995.
- [17] M. Gregory and B. Shneiderman. Shape identification in temporal data sets. In *Expanding the Frontiers of Visual Analytics and Visualization*, pages 305–321. Springer, 2012.
- [18] J. Han, J. Pei, and M. Kamber. *Data mining: concepts and techniques*. Elsevier, 2011.
- [19] M. C. Hao, M. Marwah, H. Janetzko, U. Dayal, D. A. Keim, D. Patnaik, N. Ramakrishnan, and R. K. Sharma. Visual exploration of frequent patterns in multivariate time series. *Information Visualization*, 11:71–83, 2012.
- [20] Y.-W. Huang and P. S. Yu. Adaptive query processing for time-series data. In *Proceedings of the fifth ACM SIGKDD international conference on Knowledge discovery and data mining*, pages 282–286. ACM, 1999.
- [21] R. J. L. John, N. Potti, and J. M. Patel. Ava: From data to insights through conversations. In *CIDR*, 2017.
- [22] E. Keogh and C. A. Ratanamahatana. Exact indexing of dynamic time warping. *Knowledge and information systems*, 7(3):358–386, 2005.
- [23] E. D. Kim, J. M. Lam, and J. Han. Aim: Approximate intelligent matching for time series data. In *International Conference on Data Warehousing and Knowledge Discovery*, pages 347–357. Springer, 2000.
- [24] Z. Kozareva, K. Voevodski, and S.-H. Teng. Class label enhancement via related instances. In *Proceedings of the conference on empirical methods in natural language processing*, pages 118–128. Association for Computational Linguistics, 2011.
- [25] J. Lafferty, A. McCallum, and F. C. Pereira. Conditional random fields: Probabilistic models for segmenting and labeling sequence data. 2001.
- [26] Y. Lamdan and H. J. Wolfson. Geometric hashing: A general and efficient model-based recognition scheme. 1988.
- [27] F. Li and H. Jagadish. Constructing an interactive natural language interface for relational databases. *Proceedings of the VLDB Endowment*, 8(1):73–84, 2014.
- [28] R. A. K.-I. Lin and H. S. S. K. Shim. Fast similarity search in the presence of noise, scaling, and translation in time-series databases. In *Proceeding of the 21th International Conference on Very Large Data Bases*, pages 490–501. Citeseer, 1995.
- [29] M. Mohebbi, D. Vanderkam, J. Kodysh, R. Schonberger, H. Choi, and S. Kumar. Google correlate whitepaper. 2011.
- [30] E. Morganson, R. Gruendl, F. Menanteau, M. C. Kind, Y.-C. Chen, G. Daues, A. Drlica-Wagner, D. Friedel, M. Gower, M. Johnson, et al. The dark energy survey image processing pipeline. *Publications of the Astronomical Society of the Pacific*, 130(989):074501, 2018.
- [31] P. K. e. a. Muthumanickam. Shape grammar extraction for efficient query-by-sketch pattern matching in long time series. In *Visual Analytics Science and Technology (VAST), 2016 IEEE Conference on*, pages 121–130. IEEE, 2016.
- [32] R. T. Olszewski. Generalized feature extraction for structural pattern recognition in time-series data. Technical report, CARNEGIE-MELLON UNIV PITTSBURGH PA SCHOOL OF COMPUTER SCIENCE, 2001.
- [33] J. Paparrizos and L. Gravano. k-shape: Efficient and accurate clustering of time series. In *Proceedings of the 2015 ACM SIGMOD International Conference on Management of Data*, pages 1855–1870. ACM, 2015.
- [34] R. A. G. Psaila and E. L. Wimmers Mohamed <. Querying shapes of histories. *Very Large Data Bases. Zurich, Switzerland: IEEE*, 1995.
- [35] Y. Qu, C. Wang, and X. S. Wang. Supporting fast search in time series for movement patterns in multiple scales. In *Proceedings of the seventh international conference on Information and knowledge management*, pages 251–258. ACM, 1998.
- [36] L. Rabiner, A. Rosenberg, and S. Levinson. Considerations in dynamic time warping algorithms for discrete word recognition. *IEEE Transactions on Acoustics, Speech, and Signal Processing*, 26(6):575–582, 1978.
- [37] T. Rakthanmanon, B. Campana, A. Mueen, G. Batista, B. Westover, Q. Zhu, J. Zakaria, and E. Keogh. Searching and mining trillions of time series subsequences under dynamic time warping. In *Proceedings of the 18th ACM SIGKDD international conference on Knowledge discovery and data mining*, pages 262–270. ACM, 2012.
- [38] C. A. Ralanamahatana, J. Lin, D. Gunopulos, E. Keogh, M. Vlachos, and G. Das. Mining time series data. In *Data mining and knowledge discovery handbook*, pages 1069–1103. Springer, 2005.
- [39] R. P. Roetter, C. T. Hoanh, A. G. Laborte, H. Van Keulen, M. K. Van Ittersum, C. Dreiser, C. A. Van Diepen, N. De Ridder, and H. Van Laar. Integration of systems network (sysnet) tools for regional land use scenario analysis in asia. *Environmental Modelling & Software*, 20(3):291–307, 2005.
- [40] K. Ryall, N. Lesh, T. Lanning, D. Leigh, H. Miyashita, and S. Makino. Querylines: approximate query for visual browsing. In *CHI’05 Extended Abstracts on Human Factors in Computing Systems*, pages 1765–1768. ACM, 2005.
- [41] H. Sakoe and S. Chiba. Dynamic programming algorithm optimization for spoken word recognition. *IEEE transactions on acoustics, speech, and signal processing*, 26(1):43–49, 1978.
- [42] V. Setlur, S. E. Battersby, M. Tory, R. Gossweiler, and A. X. Chang. Eviza: A natural language interface for visual analysis. In *Proceedings of the 29th Annual Symposium on User Interface Software and Technology*,

- pages 365–377. ACM, 2016.
- [43] H. Shatkay and S. B. Zdonik. Approximate queries and representations for large data sequences. In *Data Engineering, 1996. Proceedings of the Twelfth International Conference on*, pages 536–545. IEEE, 1996.
 - [44] T. Siddiqui, A. Kim, J. Lee, K. Karahalios, and A. Parameswaran. Effortless data exploration with zenvisage: an expressive and interactive visual analytics system. *Proceedings of the VLDB Endowment*, 10(4):457–468, 2016.
 - [45] T. Siddiqui, X. Ren, A. Parameswaran, and J. Han. Facetgist: Collective extraction of document facets in large technical corpora. In *Proceedings of the 25th ACM International on Conference on Information and Knowledge Management*, pages 871–880. ACM, 2016.
 - [46] R. A. Wagner, R. Tabibiazar, A. Liao, and T. Quertermous. Genome-wide expression dynamics during mouse embryonic development reveal similarities to drosophila development. *Developmental biology*, 288(2):595–611, 2005.
 - [47] M. Wattenberg. Sketching a graph to query a time-series database. In *CHI’01 Extended Abstracts on Human factors in Computing Systems*, pages 381–382. ACM, 2001.
 - [48] L. Ye and E. Keogh. Time series shapelets: a new primitive for data mining. In *Proceedings of the 15th ACM SIGKDD international conference on Knowledge discovery and data mining*, pages 947–956. ACM, 2009.